

Search for Eccentric Black Hole Coalescences during the Third Observing Run of LIGO and Virgo

A. G. ABAC,¹ R. ABBOTT,² H. ABE,³ F. ACERNESE,^{4,5} K. ACKLEY,⁶ C. ADAMCEWICZ,⁷ S. ADHICARY,⁸ N. ADHIKARI,⁹ R. X. ADHIKARI,² V. K. ADKINS,¹⁰ V. B. ADYA,¹¹ C. AFFELDT,^{12,13} D. AGARWAL,¹⁴ M. AGATHOS,¹⁵ O. D. AGUIAR,¹⁶ I. AGUILAR,¹⁷ L. AIELLO,¹⁸ A. AIN,¹⁹ P. AJITH,²⁰ T. AKUTSU,^{21,22} S. ALBANESI,^{23,24} R. A. ALFAIDI,²⁵ A. AL-JODAH,²⁶ C. ALLÉNÉ,²⁷ A. ALLOCCA,^{28,5} M. ALMUALLA,²⁹ P. A. ALTIN,¹¹ S. ÁLVAREZ-LÓPEZ,³⁰ A. AMATO,^{31,32} L. AMEZ-DROZ,³³ A. AMOROSI,³³ S. ANAND,² A. ANANYEVA,² R. ANDERSEN,³⁴ S. B. ANDERSON,² W. G. ANDERSON,² M. ANDIA,³⁵ M. ANDO,^{36,37} T. ANDRADE,³⁸ N. ANDRES,²⁷ M. ANDRÉS-CARCASONA,³⁹ T. ANDRIĆ,^{1,40} S. ANSOLDI,^{41,42} J. M. ANTELLIS,⁴³ S. ANTIER,⁴⁴ M. AOUMI,⁴⁵ T. APOSTOLATOS,⁴⁶ E. Z. APPAVURAVTHER,^{47,48} S. APPERT,² S. K. APPLE,⁴⁹ K. ARAI,² A. ARAYA,⁵⁰ M. C. ARAYA,² J. S. AREEDA,⁵¹ N. ARITOMI,⁵² F. ARMATO,⁵³ N. ARNAUD,^{35,54} M. AROGETI,⁵⁵ S. M. ARONSON,¹⁰ K. G. ARUN,⁵⁶ G. ASHTON,⁵⁷ Y. ASO,^{21,58} M. ASSIDUO,^{59,60} S. ASSIS DE SOUZA MELO,⁵⁴ S. M. ASTON,⁶¹ P. ASTONE,⁶² F. AUBIN,⁶⁰ K. AULTONEAL,⁴³ S. BABAK,⁶³ A. BADALYAN,⁶⁴ F. BADARACCO,⁵³ C. BADGER,⁶⁵ S. BAE,⁶⁶ S. BAGNASCO,²⁴ Y. BAI,² J. G. BAIER,⁶⁷ R. BAJPAI,²¹ T. BAKA,⁶⁸ M. BALL,⁶⁹ G. BALLARDIN,⁵⁴ S. W. BALLMER,⁷⁰ G. BALTUS,⁷¹ S. BANAGIRI,⁷² B. BANERJEE,⁴⁰ D. BANKAR,¹⁴ P. BARAL,⁹ J. C. BARAYOGA,² J. BARBER,¹⁸ B. C. BARISH,² D. BARKER,⁵² P. BARNEO,^{38,73} F. BARONE,^{74,5} B. BARR,²⁵ L. BARSOTTI,⁷⁵ M. BARSUGLIA,⁶³ D. BARTA,⁷⁶ S. D. BARTHELMI,⁷⁷ M. A. BARTON,²⁵ I. BARTOS,⁷⁸ S. BASAK,²⁰ A. BASALAEV,⁷⁹ R. BASSIRI,¹⁷ A. BASTI,^{80,19} M. BAWAJ,^{81,47} P. BAXI,⁸² J. C. BAYLEY,²⁵ A. C. BAYLOR,⁹ M. BAZZAN,^{83,84} B. BÉCSY,⁸⁵ V. M. BEDAKIHALE,⁸⁶ F. BEIRNAERT,⁸⁷ M. BEJGER,⁸⁸ A. S. BELL,²⁵ V. BENEDETTO,⁸⁹ D. BENIWAŁ,⁹⁰ W. BENOIT,²⁹ J. D. BENTLEY,⁷⁹ M. BEN YAALA,⁹¹ S. BERA,⁹² M. BERBEL,⁹³ F. BERGAMIN,^{12,13} B. K. BERGER,¹⁷ S. BERNUZZI,⁹⁴ M. BEROIZ,² C. P. L. BERRY,²⁵ D. BERSANETTI,⁵³ A. BERTOLINI,³² J. BETZWIENER,⁶¹ D. BEVERIDGE,²⁶ N. BEVINS,⁹⁵ R. BHANDARE,⁹⁶ A. V. BHANDARI,¹⁴ U. BHARDWAJ,^{97,32} R. BHATT,² D. BHATTACHARJEE,⁶⁷ S. BHAUMIK,⁷⁸ A. BIANCHI,^{32,98} I. A. BILENKO,⁹⁹ M. BILICKI,¹⁰⁰ G. BILLINGSLEY,² A. BINETTI,¹⁰¹ S. BINI,^{102,103} O. BIRNHOLTZ,¹⁰⁴ S. BISCANS,^{2,75} M. BISCHI,^{59,60} S. BISCOVEANU,⁷⁵ A. BISHT,¹³ M. BITOSSO,^{54,19} M.-A. BIZOUARD,⁴⁴ J. K. BLACKBURN,² C. D. BLAIR,^{26,61} D. G. BLAIR,²⁶ F. BOBBA,^{105,106} N. BODE,^{12,13} M. BOËR,⁴⁴ G. BOGAERT,⁴⁴ G. BOILEAU,^{107,44} M. BOLDRINI,^{108,62} G. N. BOLINGBROKE,⁹⁰ L. D. BONAVENA,⁸³ R. BONDARESCU,³⁸ F. BONDU,¹⁰⁹ E. BONILLA,¹⁷ G. S. BONILLA,⁵¹ R. BONNAND,²⁷ P. BOOKER,^{12,13} V. BOSCHI,¹⁹ S. BOSE,¹⁴ V. BOSSILKOV,⁶¹ V. BOUDART,⁷¹ A. BOZZI,⁵⁴ C. BRADASCHIA,¹⁹ P. R. BRADY,⁹ M. BRAGLIA,¹¹⁰ A. BRANCH,⁶¹ M. BRANCHESI,^{40,111} M. BRESCHI,⁹⁴ T. BRIANT,¹¹² A. BRILLET,⁴⁴ M. BRINKMANN,^{12,13} P. BROCKILL,⁹ A. F. BROOKS,² D. D. BROWN,⁹⁰ M. L. BROZZETTI,^{81,47} S. BRUNETT,² G. BRUNO,¹¹³ R. BRUNTZ,¹¹⁴ J. BRYANT,¹¹⁵ F. BUCCI,⁶⁰ J. BUCHANAN,¹¹⁴ O. BULASHENKO,^{38,73} T. BULIK,¹¹⁶ H. J. BULTEN,³² A. BUONANNO,^{117,1} K. BURTNKY,⁵² R. BUSCICCHIO,^{118,119} D. BUSKULIC,²⁷ C. BUY,¹²⁰ G. S. CABOURN DAVIES,¹²¹ G. CABRAS,^{41,42} R. CABRITA,¹¹³ L. CADONATI,⁵⁵ G. CAGNOLI,¹²² C. CAHILLANE,⁷⁰ H. W. CAIN III,¹⁰ J. CALDERÓN BUSTILLO,¹²³ J. D. CALLAGHAN,²⁵ T. A. CALLISTER,¹²⁴ E. CALLONI,^{28,5} J. B. CAMP,⁷⁷ M. CANEPA,^{125,53} G. CANEVA SANTORO,³⁹ M. CANNACCIUOLO,¹⁰⁵ K. C. CANNON,¹²⁶ H. CAO,³⁴ Z. CAO,¹²⁷ L. A. CAPISTRAN,¹²⁸ E. CAPOCASA,⁶³ E. CAPOTE,⁷⁰ G. CARAPELLA,^{105,106} F. CARBOGNANI,⁵⁴ M. CARLASSARA,^{12,13} J. B. CARLIN,¹²⁹ M. CARPINELLI,^{118,130,54} J. J. CARTER,^{12,13} G. CARULLO,¹³¹ J. CASANUEVA DIAZ,⁵⁴ C. CASENTINI,^{132,133} G. CASTALDI,¹³⁴ S. Y. CASTRO-LUCAS,¹³⁵ S. CAUDILL,^{32,68} M. CAVAGLIÀ,¹³⁶ R. CAVALIERI,⁵⁴ G. CELLA,¹⁹ P. CERDÁ-DURÁN,^{137,138} E. CESARINI,¹³³ W. CHAIBI,⁴⁴ S. CHALATHADKA-SUBRAHMANYA,⁷⁹ C. CHAN,¹²⁶ J. C. L. CHAN,¹²⁴ K. H. M. CHAN,¹³⁹ M. CHAN,³⁰ W. L. CHAN,¹³⁹ K. CHANDRA,¹⁴⁰ I. P. CHANG,¹⁴¹ R.-J. CHANG,¹⁴² W. CHANG,¹⁴¹ P. CHANIAL,⁶³ S. CHAO,^{141,143} C. CHAPMAN-BIRD,²⁵ E. L. CHARLTON,¹¹⁴ P. CHARLTON,¹⁴⁴ E. CHASSANDE-MOTTIN,⁶³ L. CHASTAIN,⁷ C. CHATTERJEE,²⁶ DEBARATI CHATTERJEE,¹⁴ DEEP CHATTERJEE,⁷⁵ M. CHATURVEDI,⁹⁶ S. CHATY,⁶³ K. CHATZIOANNOU,² A. CHEN,¹⁴⁵ A. H.-Y. CHEN,¹⁴⁶ D. CHEN,¹⁴⁷ H. CHEN,¹⁴¹ H. Y. CHEN,¹⁴⁸ J. CHEN,⁷⁵ K. H. CHEN,¹⁴³ X. CHEN,²⁶ Y.-R. CHEN,¹⁴¹ Y. CHEN,¹⁴⁹ H. CHENG,⁷⁸ P. CHESSA,^{80,19} H. Y. CHIA,⁷⁸ F. CHIADINI,^{150,106} C. CHIANG,¹⁴³ G. CHIARINI,⁸⁴ A. CHIBA,¹⁵¹ R. CHIBA,¹⁵² R. CHERICI,¹⁵³ A. CHINCARINI,⁵³ M. L. CHIOFALO,^{80,19} A. CHIUMMO,⁵⁴ C. CHOU,¹⁴⁶ S. CHOUDHARY,²⁶ N. CHRISTENSEN,⁴⁴ S. S. Y. CHUA,¹¹ K. W. CHUNG,⁶⁵ G. CIANI,^{83,84} P. CIECIELAG,⁸⁸ M. CIEŚLAR,⁸⁸ M. CIFALDI,^{132,133} A. A. CIOBANU,⁹⁰ R. CIOLFI,^{154,84} F. CLARA,⁵² J. A. CLARK,^{2,55} T. A. CLARKE,⁷ P. CLEARWATER,¹⁵⁵ S. CLESSE,¹⁵⁶ F. CLEVA,⁴⁴ E. COCCIA,^{40,111,39} E. CODAZZO,⁴⁰ P.-F. COHADON,¹¹² M. COLLEONI,⁹² C. G. COLLETTE,³³ J. COLLINS,⁶¹ A. COLOMBO,^{118,119,157} M. COLPI,^{118,119} C. M. COMPTON,⁵² L. CONTI,⁸⁴ S. J. COOPER,¹¹⁵ T. R. CORBITT,¹⁰ I. CORDERO-CARRIÓN,¹⁵⁸ S. COREZZI,^{81,47} N. J. CORNISH,⁸⁵ A. CORSI,¹⁵⁹ S. CORTESE,⁵⁴ C. A. COSTA,¹⁶ R. COTTINGHAM,⁶¹ M. W. COUGHLIN,²⁹ A. COUINEAUX,⁶² J.-P. COULON,⁴⁴ S. T. COUNTRYMAN,¹⁶⁰ J.-F. COUPECHOUX,¹⁵³ B. COUSINS,⁸ P. COUVARES,^{2,55} D. M. COWARD,²⁶ M. J. COWART,⁶¹ B. D. COWBURN,¹⁶¹ D. C. COYNE,² R. COYNE,¹⁶² K. CRAIG,⁹¹ J. D. E. CREIGHTON,⁹ T. D. CREIGHTON,¹⁶³ A. W. CRISWELL,²⁹ J. C. G. CROCKETT-GRAY,¹⁰ M. CROQUETTE,¹¹² R. CROUCH,⁵² S. G. CROWDER,¹⁶⁴ J. R. CUDELL,⁷¹ T. J. CULLEN,² A. CUMMING,²⁵ E. CUOCO,^{54,165,19} M. CURYŁO,¹¹⁶ M. CUSINATO,¹³⁷ P. DABADIE,¹²² T. DAL CANTON,³⁵ S. DALL'OSSO,⁶² G. DÁLYA,⁸⁷ B. D'ANGELO,⁵³ S. DANILISHIN,^{31,32} S. D'ANTONIO,¹³³ K. DANZMANN,^{13,12,13} K. E. DARROCH,¹¹⁴ C. DARSOW-FROMM,⁷⁹ L. P. DARTEZ,⁵² A. DASGUPTA,⁸⁶ S. DATTA,⁵⁶ V. DATTILO,⁵⁴ A. DAUMAS,⁶³ I. DAVE,⁹⁶ A. DAVENPORT,¹³⁵ M. DAVIER,³⁵ D. DAVIS,² M. C. DAVIS,⁹⁵ E. J. DAW,¹⁶⁶ M. DAX,¹ M. DEENADAYALAN,¹⁴ J. DEGALLAIX,¹⁶⁷ M. DE LAURENTIS,^{28,5} S. DELÉGLISE,¹¹² V. DEL FAVERO,⁷⁷ F. DE LILLO,¹¹³ D. DELL'AQUILA,^{168,130} W. DEL POZZO,^{80,19} F. DE MARCO,^{62,108} F. DE MATTEIS,^{132,133} V. D'EMILIO,¹⁸ N. DEMOS,⁷⁵ T. DENT,¹²³ A. DEPASSE,¹¹³ R. DE PIETRI,^{169,170} R. DE ROSA,^{28,5} C. DE ROSSI,⁵⁴

- R. DE SIMONE,¹⁵⁰ S. DHURANDHAR,¹⁴ R. DIAB,⁷⁸ P. Z. DIAMOND,⁶⁷ M. C. DÍAZ,¹⁶³ N. A. DIDIO,⁷⁰ T. DIETRICH,¹
 L. DI FIORE,⁵ C. DI FRONZO,³³ F. DI GIOVANNI,¹³⁷ M. DI GIOVANNI,⁴⁰ T. DI GIROLAMO,^{28,5} D. DIKSHA,^{32,31}
 A. DI LIETO,^{80,19} A. DI MICHELE,⁸¹ J. DING,^{63,171} S. DI PACE,^{108,62} I. DI PALMA,^{108,62} F. DI RENZO,¹⁵³ DIVYAJYOTI,¹⁷²
 A. DMITRIEV,¹¹⁵ Z. DOCTOR,⁷² E. DOHMEN,⁵² P. P. DOLEVA,¹¹⁴ L. DONAHUE,¹⁷³ L. D'ONOFRIO,^{28,5} F. DONOVAN,⁷⁵
 K. L. DOOLEY,¹⁸ T. DOONEY,⁶⁸ S. DORAVARI,¹⁴ O. DOROSH,¹⁷⁴ M. DRAGO,^{108,62} J. C. DRIGGERS,⁵² Y. DRORI,² H. DU,³⁰
 J.-G. DUCOIN,^{175,63} L. DUNN,¹²⁹ U. DUPLIETS,⁴⁰ D. D'URSO,^{168,130} H. DUVAL,¹⁷⁶ P.-A. DUVERNE,³⁵ S. E. DWYER,⁵²
 C. EASSA,⁵² M. EBERSOLD,^{177,27} T. ECKHARDT,⁷⁹ G. EDDOLLS,²⁵ B. EDELMAN,⁶⁹ T. B. EDO,² O. EDY,¹²¹ A. EFFLER,⁶¹
 J. EICHHOLZ,¹¹ H. EINSLE,⁴⁴ M. EISENMANN,²¹ R. A. EISENSTEIN,⁷⁵ A. EJLLI,¹⁸ E. ENGELBY,⁵¹ A. J. ENGL,¹⁷
 L. ERRICO,^{28,5} R. C. ESSICK,¹⁷⁸ H. ESTELLÉS,¹ D. ESTEVEZ,¹⁷⁹ T. ETZEL,² C. R. EVANS,¹⁸ M. EVANS,⁷⁵ T. M. EVANS,⁶¹
 T. EVSTAFYEVA,¹⁵ B. E. EWING,⁸ J. M. EZQUIAGA,¹²⁴ F. FABRIZI,^{59,60} F. FAEDI,^{60,59} V. FAFONE,^{132,133,40} H. FAIR,⁷⁰
 S. FAIRHURST,¹⁸ P. C. FAN,¹⁷³ A. M. FARAH,¹²⁴ B. FARR,⁶⁹ W. M. FARR,^{180,181} E. J. FAUCHON-JONES,¹⁸ G. FAVARO,⁸³
 M. FAVATA,¹⁸² M. FAYS,⁷¹ J. FEICHT,² M. M. FEJER,¹⁷ E. FENYVESI,^{76,183} D. L. FERGUSON,¹⁴⁸ I. FERRANTE,^{80,19}
 T. A. FERREIRA,¹⁶ F. FIDECARO,^{80,19} A. FIORI,^{19,80} I. FIORI,⁵⁴ M. FISHBACH,¹⁷⁸ R. P. FISHER,¹¹⁴ R. FITTIPALDI,^{184,106}
 V. FIUMARA,^{185,106} R. FLAMINIO,²⁷ S. M. FLEISCHER,¹⁸⁶ L. S. FLEMING,¹⁸⁷ E. FLODEN,²⁹ H. FONG,³⁰ J. A. FONT,^{137,138}
 B. FORNAL,¹⁸⁸ P. W. F. FORSYTH,¹¹ K. FRANCESCHETTI,¹⁶⁹ A. FRANKE,⁷⁹ S. FRASCA,^{108,62} F. FRASCONI,¹⁹
 A. FRATTALE MASCIOLI,^{108,62} Z. FREI,¹⁸⁹ A. FREISE,^{32,98} O. FREITAS,^{190,137} R. FREY,⁶⁹ W. FRISCHERTZ,⁶¹
 P. FRITSCHEL,⁷⁵ V. V. FROLOV,⁶¹ G. G. FRONZÉ,²⁴ S. FUJII,¹⁵² I. FUKUNAGA,¹⁹¹ P. FULDA,⁷⁸ M. FYFFE,⁶¹
 W. E. GABELLA,¹⁹² B. GADRE,⁶⁸ J. R. GAIR,¹ J. GAIS,¹³⁹ S. GALAUDAGE,⁷ S. GALLARDO,¹⁹³ R. GAMBA,⁹⁴
 D. GANAPATHY,⁷⁵ A. GANGULY,¹⁴ S. G. GAONKAR,¹⁴ B. GARAVENTA,^{53,125} J. GARCIA-BELLIDO,¹¹⁰ C. GARCÍA-NÚÑEZ,¹⁸⁷
 C. GARCÍA-QUIRÓS,⁹² J. W. GARDNER,¹¹ K. A. GARDNER,³⁰ J. GARGIULO,⁵⁴ F. GARUFI,^{28,5} C. GASBARRA,^{132,133}
 B. GATELEY,⁵² V. GAYATHRI,⁹ G. GEMME,⁵³ A. GENNAI,¹⁹ J. GEORGE,⁹⁶ O. GERBERDING,⁷⁹ L. GERGELY,¹⁹⁴ N. GHADIRI,⁵¹
 ABHIRUP GHOSH,¹ ARCHISMAN GHOSH,⁸⁷ SHAON GHOSH,¹⁸² SHROBANA GHOSH,^{12,13} SUPROVO GHOSH,¹⁴
 TATHAGATA GHOSH,¹⁴ L. GIACOPPO,^{108,62} J. A. GIAIME,^{10,61} K. D. GIARDINA,⁶¹ D. R. GIBSON,¹⁸⁷ C. GIER,⁹¹ P. GIRI,^{19,80}
 F. GISSI,⁸⁹ S. GKAITATZIS,⁸⁰ J. GLANZER,¹⁰ A. E. GLECKL,⁵¹ F. GLOTIN,³⁵ J. GODFREY,⁶⁹ P. GODWIN,² E. GOETZ,³⁰
 R. GOETZ,⁷⁸ J. GOLOMB,² S. GOMEZ LOPEZ,^{108,62} B. GONCHAROV,⁴⁰ G. GONZÁLEZ,¹⁰ A. W. GOODWIN-JONES,²⁶
 M. GOSSELIN,⁵⁴ R. GOUATY,²⁷ D. W. GOULD,¹¹ S. GOYAL,²⁰ B. GRACE,¹¹ A. GRADO,^{195,5} V. GRAHAM,²⁵
 A. E. GRANADOS,²⁹ M. GRANATA,¹⁶⁷ V. GRANATA,¹⁰⁵ S. GRAS,⁷⁵ P. GRASSIA,² C. GRAY,⁵² R. GRAY,²⁵ G. GRECO,⁴⁷
 A. C. GREEN,⁹⁸ S. M. GREEN,¹²¹ S. R. GREEN,¹ A. M. GRETARSSON,⁴³ E. M. GRETARSSON,⁴³ D. GRIFFITH,²
 W. L. GRIFFITHS,¹⁸ H. L. GRIGGS,⁵⁵ G. GRIGNANI,^{81,47} A. GRIMALDI,^{102,103} C. GRIMAUD,²⁷ H. GROTE,¹⁸ A. S. GRUSON,⁵¹
 D. GUERRA,¹³⁷ D. GUETTA,⁶² G. M. GUIDI,^{59,60} A. R. GUIMARAES,¹⁰ H. K. GULATI,⁸⁶ F. GULMINELLI,^{196,197}
 A. M. GUNNY,⁷⁵ H. GUO,¹⁸⁸ Y. GUO,^{32,31} ANCHAL GUPTA,² ANURADHA GUPTA,¹⁹⁸ ISH GUPTA,⁸ N. C. GUPTA,⁸⁶
 P. GUPTA,^{32,68} S. K. GUPTA,¹⁴⁰ N. GUPTA,¹ R. GURAV,³⁴ J. GURS,⁷⁹ E. K. GUSTAFSON,² N. GUTIERREZ,¹⁶⁷ F. GUZMAN,¹²⁸
 D. HABA,³ L. HAEGEL,⁶³ G. HAIN,¹¹⁴ S. HAINO,¹⁹⁹ O. HALIM,⁴² E. D. HALL,⁷⁵ E. Z. HAMILTON,¹⁷⁷ G. HAMMOND,²⁵
 W.-B. HAN,²⁰⁰ M. HANEY,^{177,32} J. HANKS,⁵² C. HANNA,⁸ M. D. HANNAM,¹⁸ O. A. HANNUKSELA,¹³⁹ A. G. HANSELMAN,¹²⁴
 H. HANSEN,⁵² J. HANSON,⁶¹ R. HARADA,¹²⁶ T. HARDER,⁴⁴ K. HARIS,^{32,68} T. HARMARK,¹³¹ J. HARMS,^{40,111} G. M. HARRY,⁴⁹
 I. W. HARRY,¹²¹ D. HARTWIG,⁷⁹ B. HASKELL,⁸⁸ C.-J. HASTER,²⁰¹ J. S. HATHAWAY,¹⁶¹ K. HAUGHIAN,²⁵ H. HAYAKAWA,⁴⁵
 K. HAYAMA,²⁰² F. J. HAYES,²⁵ J. HEALY,¹⁶¹ A. HEFFERNAN,⁹² A. HEIDMANN,¹¹² M. C. HEINTZE,⁶¹ J. HEINZE,¹¹⁵
 J. HEINZEL,⁷⁵ H. HEITMANN,⁴⁴ F. HELLMAN,²⁰³ P. HELLO,³⁵ A. F. HELMLING-CORNELL,⁶⁹ G. HEMMING,⁵⁴ M. HENDRY,²⁵
 I. S. HENG,²⁵ E. HENNES,³² J.-S. HENNIG,^{31,32} M. HENNIG,^{31,32} C. HENSHAW,⁵⁵ A. HERNANDEZ,¹⁸² T. HERTOG,¹⁰¹
 M. HEURS,^{12,13} A. L. HEWITT,^{15,204} S. HIGGINBOTHAM,¹⁸ S. HILD,^{31,32} P. HILL,⁹¹ Y. HIMEMOTO,²⁰⁵ A. S. HINES,¹²⁸
 N. HIRATA,²¹ C. HIROSE,²⁰⁶ J. HO,¹⁴³ S. HOANG,³⁵ S. HOCHHEIM,^{12,13} D. HOFMAN,¹⁶⁷ J. N. HOHMANN,⁷⁹
 N. A. HOLLAND,^{32,98} K. HOLLEY-BOCKELMANN,¹⁹² I. J. HOLLOWES,¹⁶⁶ Z. J. HOLMES,⁹⁰ D. E. HOLZ,¹²⁴ C. HONG,¹⁷
 Q. HONG,¹⁴¹ J. HORNUNG,⁶⁹ S. HOSHINO,²⁰⁶ J. HOUGH,²⁵ S. HOURIHANE,² E. J. HOWELL,²⁶ C. G. HOY,¹²¹ D. HOYLAND,¹¹⁵
 H.-F. HSIEH,¹⁴¹ C. HSIUNG,²⁰⁷ H. C. HSU,¹⁴³ S.-C. HSU,^{208,141} W.-F. HSU,¹⁰¹ P. HU,¹⁹² Q. HU,²⁵ H. Y. HUANG,¹⁴³
 Y.-J. HUANG,⁸ Y. HUANG,⁷⁵ Y. T. HUANG,²⁰⁸ M. T. HÜBNER,¹²⁹ A. D. HUDDART,²⁰⁹ B. HUGHEY,⁴³ D. C. Y. HUI,²¹⁰
 V. HUI,²⁷ R. HUR,⁶⁹ S. HUSA,⁹² R. HUXFORD,⁸ T. HUYNH-DINH,⁶¹ J. HYLAND,²⁵ A. IAKOVLEV,²¹¹ G. A. IANDOLO,³¹
 A. IESS,^{165,19} K. INAYOSHI,²¹² Y. INOUE,¹⁴³ G. IORIO,⁸³ P. IOSIF,²¹³ J. IRWIN,²⁵ M. ISI,^{180,181} M. A. ISMAIL,¹⁴³
 Y. ITOH,^{191,214} M. IWAYA,¹⁵² B. R. IYER,²⁰ V. JABERIANHAMEDAN,²⁶ T. JACQMIN,¹¹² P.-E. JACQUET,¹¹² S. J. JADHAV,²¹⁵
 S. P. JADHAV,¹⁵⁵ D. JAIN,⁷ T. JAIN,¹⁵ A. L. JAMES,¹⁸ P. A. JAMES,¹¹⁴ R. JAMSHIDI,³³ A. Z. JAN,¹⁴⁸ K. JANI,¹⁹²
 L. JANIUREK,²⁵ J. JANQUART,^{68,32} K. JANSSENS,^{107,44} N. N. JANTHALUR,²¹⁵ S. JARABA,¹¹⁰ P. JARANOWSKI,²¹⁶ S. JAROV,³⁰
 P. JASAL,³⁸ R. JAUME,⁹² W. JAVED,¹⁸ K. JENNER,⁹⁰ A. JENNINGS,⁵² W. JIA,⁷⁵ J. JIANG,⁷⁸ H.-B. JIN,^{217,218}
 K. JOHANSMEYER,¹⁸² G. R. JOHNS,¹¹⁴ N. A. JOHNSON,⁷⁸ R. JOHNSTON,²⁵ N. JOHNY,^{12,13} D. H. JONES,¹¹ D. I. JONES,²¹⁹
 R. JONES,²⁵ P. JOSHI,⁸ L. JU,²⁶ K. JUNG,²²⁰ J. JUNKER,^{12,13} V. JUSTE,¹⁷⁹ T. KAJITA,¹⁵² C. KALAGHATGI,^{68,32,221}
 V. KALOGERA,⁷² M. KAMIIZUMI,⁴⁵ N. KANDA,^{214,191} S. KANDHASAMY,¹⁴ G. KANG,²²² J. B. KANNER,² S. J. KAPADIA,¹⁴
 D. P. KAPASI,¹¹ S. KARAT,² C. KARATHANASIS,³⁹ S. KARKI,¹³⁶ T. KARYDAS,²⁷ Y. A. KAS-DANOUCHE,⁶⁴ R. KASHYAP,⁸
 M. KASPRZACK,² W. KASTAUN,^{12,13} J. KATO,¹⁵¹ T. KATO,¹⁵² S. KATSANEVAS,^{54,*} E. KATSAVOUNIDIS,⁷⁵ J. K. KATSUREN,⁶⁴
 W. KATZMAN,⁶¹ T. KAUR,²⁶ K. KAWABE,⁵² F. KÉFÉLIAN,⁴⁴ D. KEITEL,⁹² J. KELLEY-DERZON,⁷⁸ S. A. KEMPER,⁴³
 J. KENNINGTON,⁸ R. KESHARWANI,¹⁴ J. S. KEY,²²³ S. KHADKA,¹⁷ F. Y. KHALILI,⁹⁹ T. KHANAM,¹⁵⁹ E. A. KHAZANOV,²¹¹
 M. KHURSHEED,⁹⁶ N. KIJUNCHOO,¹¹ C. KIM,²²⁴ J. C. KIM,²²⁵ K. KIM,²²⁴ M. H. KIM,²²⁶ P. KIM,²²⁶ S. KIM,²¹⁰
 W. S. KIM,²²⁷ Y.-M. KIM,²²⁸ C. KIMBALL,⁷² N. KIMURA,⁴⁵ M. KINLEY-HANLON,²⁵ R. KIRCHHOFF,^{12,13} J. S. KISSEL,⁵²
 T. KIYOTA,¹⁹¹ S. KLIMENKO,⁷⁸ T. KLINGER,¹⁸ A. M. KNEE,³⁰ N. KNUST,^{12,13} P. KOCH,^{12,13} S. M. KOEHLLENBECK,¹⁷
 G. KOEKOEK,^{32,31} K. KOHRI,²²⁹ K. KOKEYAMA,¹⁸ S. KOLEY,⁴⁰ N. D. KOLIADKO,⁶⁴ P. KOLITSIDOU,¹⁸ M. KOLSTEIN,³⁹

- K. KOMORI,¹²⁶ V. KONDRASHOV,² A. K. H. KONG,¹⁴¹ A. KONTOS,²³⁰ M. KOROBKO,⁷⁹ R. V. KOSSAK,^{12,13} N. KOVATSOS,⁶⁵
M. KOVALAM,²⁶ N. KOYAMA,²⁰⁶ D. B. KOZAK,² S. L. KRANZHOF, ^{31,32,12,13} V. KRINGEL,^{12,13} N. V. KRISHNENDU,²⁰
A. KRÓLAK,^{231,174} G. KUEHN,^{12,13} P. KUIJER,³² S. KULKARNI,¹⁹⁸ A. KULUR RAMAMOCHAN,¹¹ A. KUMAR,²¹⁵
PRAVEEN KUMAR,¹²³ PRAYUSH KUMAR,²⁰ RAHUL KUMAR,⁵² RAKESH KUMAR,⁸⁶ J. KUME,¹²⁶ K. KUNS,⁷⁵
S. KUROYANAGI,^{110,232} S. KUWAHARA,¹²⁶ K. KWAK,²²⁰ K. KWAN,¹¹ G. LACAILLE,²⁵ P. LAGABBE,²⁷ D. LAGHI,¹²⁰ S. LAI,¹⁴⁶
M. H. LAKKIS,³³ E. LALANDE,²³³ M. LALLEMAN,¹⁰⁷ A. LAMBERTS,^{44,234} M. LANDRY,⁵² B. B. LANE,⁷⁵ R. N. LANG,⁷⁵
J. LANGE,¹⁴⁸ B. LANTZ,¹⁷ A. LA RANA,⁶² I. LA ROSA,^{108,27} A. LARTAUX-VOLLARD,³⁵ P. D. LASKY,⁷ J. LAWRENCE,¹⁵⁹
M. LAXEN,⁶¹ A. LAZZARINI,² C. LAZZARO,^{83,84} P. LEACI,^{108,62} S. LEAVEY,^{12,13} S. LEBOHEC,¹⁸⁸ Y. K. LECOEUUCHE,³⁰
H. M. LEE,²²⁵ H. W. LEE,²³⁵ K. LEE,²²⁶ R.-K. LEE,¹⁴¹ R. LEE,⁷⁵ S. LEE,²³⁶ Y. LEE,¹⁴³ I. N. LEGRED,² J. LEHMANN,^{12,13}
L. LEHNER,²³⁷ A. LEMAÎTRE,²³⁸ M. LENTI,^{60,239} M. LEONARDI,^{240,21} E. LEONOVA,⁹⁷ N. LEROY,³⁵ M. LESOVSKY,²
N. LETENDRE,²⁷ M. LETHUILLIER,¹⁵³ C. LEVESQUE,²³³ Y. LEVIN,⁷ K. LEYDE,⁶³ A. K. Y. LI,² K. L. LI,¹⁴²
T. G. F. LI,^{139,101} X. LI,¹⁴⁹ CHIEN-YU LIN,^{143,141} CHUN-YU LIN,²⁴¹ E. T. LIN,¹⁴¹ F. LIN,¹⁴³ H. LIN,¹⁴³ L. C.-C. LIN,¹⁴²
Y. LIN,⁴³ F. LINDE,^{221,32} S. D. LINKER,^{134,193} T. B. LITTENBERG,²⁴² A. LIU,¹³⁹ G. C. LIU,²⁰⁷ JIAN LIU,²⁶ F. LLAMAS,¹⁶³
R. K. L. LO,² T. LO,¹⁴¹ J.-P. LOCQUET,¹⁰¹ L. LONDON,⁹⁷ A. LONGO,^{59,60} D. LOPEZ,¹⁷⁷ M. LOPEZ PORTILLA,⁶⁸
M. LORENZINI,^{132,133} V. LORIETTE,³⁵ M. LORMAND,⁶¹ G. LOSURDO,¹⁹ T. P. LOTT,⁵⁵ J. D. LOUGH,^{12,13} H. A. LOUGHLIN,⁷⁵
C. O. LOUSTO,¹⁶¹ G. LOVELACE,⁵¹ M. J. LOWRY,¹¹⁴ H. LÜCK,^{13,12,13} D. LUMACA,^{132,133} A. P. LUNDGREN,¹²¹
A. W. LUSSIER,²³³ J. E. LYNAM,¹¹⁴ L.-T. MA,¹⁴¹ S. MA,¹⁴⁹ M. MA'ARIF,¹⁴³ R. MACAS,¹²¹ M. MACINNIS,⁷⁵
D. M. MACLEOD,¹⁸ I. A. O. MACMILLAN,² A. MACQUET,³⁹ K. MAEDA,¹⁵¹ S. MAENAUT,¹⁰¹ I. MAGAÑA HERNANDEZ,⁹
C. MAGAZZÙ,¹⁹ R. M. MAGEE,² R. MAGGIORE,^{32,98} M. MAGNOZZI,^{53,125} M. MAHESH,⁷⁹ S. MAHESH,²⁴³ M. MAINI,¹⁶²
S. MAJHI,¹⁴ E. MAJORANA,^{108,62} C. N. MAKAREM,² S. MALIAKAL,² A. MALIK,⁹⁶ N. MAN,⁴⁴ V. MANDIC,²⁹
V. MANGANO,^{62,108} B. MANNIX,⁶⁹ G. L. MANSELL,^{70,75} G. MANSINGH,⁴⁹ M. MANSKE,⁹ M. MANTOVANI,⁵⁴ M. MAPELLI,^{83,84}
F. MARCHESONI,^{48,47,244} D. MARÍN PINA,^{38,73,245} F. MARION,²⁷ S. MÁRKA,¹⁶⁰ Z. MÁRKA,¹⁶⁰ C. MARKAKIS,¹⁴⁵
A. S. MARKOSYAN,¹⁷ A. MARKOWITZ,² E. MAROS,² A. MARQUINA,¹⁵⁸ S. MARSAT,^{159,60} F. MARTELLI,^{59,60} I. W. MARTIN,²⁵
R. M. MARTIN,¹⁸² B. B. MARTINEZ,¹²⁸ M. MARTINEZ,^{39,246} V. A. MARTINEZ,⁷⁸ V. MARTINEZ,¹²² K. MARTINOVIC,⁶⁵
D. V. MARTYNOV,¹¹⁵ E. J. MARX,⁷⁵ H. MASALEHDAN,⁷⁹ A. MASSEROT,²⁷ M. MASSO-REID,²⁵ M. MASTRODICASA,⁶²
S. MASTROGIOVANNI,⁶² M. MATEU-LUCENA,⁹² M. MATIUSHECHKINA,^{12,13} M. MATSUYAMA,¹⁹¹ N. MAVALVALA,⁷⁵
N. MAXWELL,⁵² G. MCCARROL,⁶¹ R. MCCARTHY,⁵² D. E. MCCLELLAND,¹¹ S. MCCORMICK,⁶¹ L. MCCULLER,²
G. I. MCGHEE,²⁵ J. MCGINN,²⁵ M. MCHEDLIDZE,¹⁸² C. MCISAAC,¹²¹ J. MCIVER,³⁰ K. MCKINNEY,¹⁶⁴ A. MCLEOD,²⁶
T. MCRAE,¹¹ S. T. MCWILLIAMS,²⁴³ D. MEACHER,⁹ M. MEHMET,^{12,13} A. K. MEHTA,¹ Q. MEIJER,⁶⁸ A. MELATOS,¹²⁹
S. MELLAERTS,¹⁰¹ A. MENENDEZ-VAZQUEZ,³⁹ C. S. MENONI,¹³⁵ R. A. MERCER,⁹ L. MERENI,¹⁶⁷ K. MERFELD,⁶⁹
E. L. MERILH,⁶¹ J. D. MERRITT,⁶⁹ M. MERZOUGUI,⁴ C. MESSENGER,²⁵ C. MESSICK,⁷⁵ M. MEYER-CONDE,¹⁹¹
F. MEYLAHN,^{12,13} A. MHASKE,¹⁴ A. MIANI,^{102,103} H. MIAO,²⁴⁷ I. MICHALOLIAKOS,⁷⁸ C. MICHEL,¹⁶⁷ Y. MICHIMURA,^{2,126}
H. MIDDLETON,¹¹⁵ D. P. MIHAYLOV,¹ A. L. MILLER,³² A. MILLER,¹⁹³ B. MILLER,^{97,32} S. MILLER,² M. MILLHOUSE,⁵⁵
E. MILOTTI,^{248,42} Y. MINENKOV,¹³³ N. MIO,²⁴⁹ LL. M. MIR,³⁹ L. MIRASOLA,^{250,62} M. MIRAVET-TENÉS,¹³⁷
C. . MIRITESCU,³⁹ A. MISHKIN,⁷⁸ A. MISHRA,¹⁴ C. MISHRA,¹⁷² T. MISHRA,⁷⁸ T. MISTRY,¹⁶⁶ A. L. MITCHELL,^{32,98}
S. MITRA,¹⁴ V. P. MITROFANOV,⁹⁹ G. MITSELMAKHER,⁷⁸ R. MITTLEMAN,⁷⁵ O. MIYAKAWA,⁴⁵ S. MIYAMOTO,¹⁵²
S. MIYOKI,⁴⁵ G. MO,⁷⁵ L. MOBILIA,^{59,60} L. M. MODAFFERI,⁹² S. R. P. MOHAPATRA,² S. R. MOHITE,⁹ M. MOLINA-RUIZ,²⁰³
C. MONDAL,¹⁹⁶ M. MONDIN,¹⁹³ M. MONTANI,^{59,60} C. J. MOORE,¹¹⁵ M. MORALES,⁵¹ D. MORARU,⁵² F. MORAWSKI,⁸⁸
A. MORE,¹⁴ S. MORE,¹⁴ C. MORENO,⁴³ G. MORENO,⁵² S. MORISAKI,^{126,152} Y. MORIWAKI,¹⁵¹ G. MORRAS,¹¹⁰
A. MOSCATELLO,⁸³ B. MOURS,¹⁷⁹ C. M. MOW-LOWRY,^{32,98} S. MOZZON,¹²¹ F. MUCIACCIA,^{108,62} ARUNAVA MUKHERJEE,²⁵¹
D. MUKHERJEE,²⁴² SOMA MUKHERJEE,¹⁶³ SUBROTO MUKHERJEE,⁸⁶ SUVODIP MUKHERJEE,^{252,237,97} N. MUKUND,^{12,13}
A. MULLAVEY,⁶¹ J. MUNCH,⁹⁰ E. A. MUÑIZ,⁷⁰ M. MURAKOSHI,²⁵³ P. G. MURRAY,²⁵ S. MUUSSE,⁹⁰ S. L. NADJI,^{12,13}
A. NAGAR,^{24,254} T. NAGAR,⁷ N. NAGARAJAN,²⁵ K. NAKAMURA,²¹ H. NAKANO,²⁵⁵ M. NAKANO,⁶¹ V. NAPOLANO,⁵⁴
I. NARDECCHIA,^{132,133} T. NARIKAWA,¹⁵² H. NAROLA,⁶⁸ L. NATICCHIONI,⁶² R. K. NAYAK,²⁵⁶ B. F. NEIL,²⁶ J. NELSON,^{89,106}
A. NELSON,¹²⁸ T. J. N. NELSON,⁶¹ M. NERY,^{12,13} S. NESSERIS,¹¹⁰ A. NEUNZERT,⁵² K. Y. NG,⁷⁵ S. W. S. NG,⁹⁰
C. NGUYEN,⁶³ P. NGUYEN,⁶⁹ L. NGUYEN QUYNH,²⁵⁷ S. A. NICHOLS,¹⁰ G. NIERADKA,⁸⁸ A. NIKO,¹⁴³ Y. NISHINO,^{21,258}
A. NISHIZAWA,¹²⁶ S. NISSANKE,^{97,32} E. NITOGIJA,¹⁵³ W. NIU,⁸ F. NOCERA,⁵⁴ M. NORMAN,¹⁸ C. NORTH,¹⁸
J. NOVAK,^{259,260,261,262} J. F. NUÑO SILES,¹¹⁰ G. NURBEK,¹⁶³ L. K. NUTTALL,¹²¹ K. OBAYASHI,²⁵³ J. OBERLING,⁵²
J. O'DELL,²⁰⁹ E. OELKER,²⁵ M. OERTEL,^{259,260,261,263,262} A. OFFERMANS,¹⁰¹ G. OGANESYAN,^{40,111} J. J. OH,²²⁷ K. OH,²¹⁰
S. H. OH,²²⁷ T. O'HANLON,⁶¹ M. OHASHI,⁴⁵ M. OHKAWA,²⁰⁶ F. OHME,^{12,13} H. OHTA,¹²⁶ A. S. OLIVEIRA,¹⁶⁰
R. OLIVERI,^{259,260,261} V. OLOWORARAN,²⁶ B. O'NEAL,¹¹⁴ K. OOHARA,^{264,265} B. O'REILLY,⁶¹ R. G. ORMISTON,²⁹
N. D. ORMSBY,¹¹⁴ M. ORSELLI,^{47,81} R. O'SHAUGHNESSY,¹⁶¹ Y. OSHIMA,²⁶⁶ S. OSHINO,⁴⁵ S. OSSOKINE,¹ C. OSTHELDER,²
D. J. OTTAWAY,⁹⁰ A. OUZRIAT,¹⁵³ H. OVERMIER,⁶¹ A. E. PACE,⁸ R. PAGANO,¹⁰ M. A. PAGE,²¹ A. PAI,¹⁴⁰ S. A. PAI,⁹⁶
A. PAL,²⁶⁷ S. PAL,²⁵⁶ O. PALASHOV,²¹¹ M. PÁLFI,¹⁸⁹ C. PALOMBA,⁶² K.-C. PAN,¹⁴¹ P. K. PANDA,²¹⁵ L. PANEBIANCO,^{59,60}
P. T. H. PANG,^{32,68} F. PANNARALE,^{108,62} B. C. PANT,⁹⁶ F. H. PANTHER,²⁶ C. D. PANZER,²⁹ F. PAOLETTI,¹⁹ A. PAOLI,⁵⁴
A. PAOLONE,^{62,268} E. E. PAPALEXAKIS,³⁴ L. PAPALINI,^{19,80} G. PAPPAS,²¹³ A. PARISI,^{32,97} J. PARK,²³⁶ W. PARKER,⁶¹
D. PASCUCCI,⁸⁷ A. PASQUALETTI,⁵⁴ R. PASSAQUIETI,^{80,19} D. PASSUELLO,¹⁹ M. PATEL,¹¹⁴ D. PATHAK,¹⁴ M. PATHAK,⁹⁰
A. PATRA,¹⁸ B. PATRICELLI,^{80,19} A. S. PATRON,¹⁰ S. PAUL,⁶⁹ E. PAYNE,² T. PEARCE,¹⁸ M. PEDRAZA,² R. PEGNA,¹⁹
M. PEGORARO,⁸⁴ A. PELE,² F. E. PEÑA ARELLANO,⁴⁵ S. PENN,²⁶⁹ A. PEREGO,^{102,103} A. PEREIRA,¹²² C. J. PEREZ,⁵²
J. J. PEREZ,⁷⁸ L. H. PEREZ,⁴³ C. PÉRIGOIS,^{154,84,83} C. C. PERKINS,⁷⁸ A. PERRECA,^{102,103} J. PERRET,⁶³ S. PERRIÈS,¹⁵³
J. W. PERRY,^{32,98} D. PESIOS,²¹³ J. PETERMANN,⁷⁹ C. PETRILLO,⁸¹ H. P. PFEIFFER,¹ H. PHAM,⁶¹ K. A. PHAM,²⁹
K. S. PHUKON,^{32,221} H. PHURAILATPAM,¹³⁹ O. J. PICCINI,³⁹ M. PICHOT,⁴⁴ M. PIENDIBENE,^{80,19} F. PIERGIOVANNI,^{59,60}

- L. PIERINI,^{108,62} G. PIERRA,¹⁵³ V. PIERRO,^{89,106} M. PIETRZAK,⁸⁸ G. PILLANT,⁵⁴ M. PILLAS,³⁵ F. PILO,¹⁹ L. PINARD,¹⁶⁷
C. PINEDA-BOSQUE,¹⁹³ I. M. PINTO,^{89,106,270,28,54} M. PINTO,⁵⁴ B. J. PIOTRZKOWSKI,⁹ M. PIRELLO,⁵² M. D. PITKIN,^{15,204,25}
A. PLACIDI,^{47,81} E. PLACIDI,^{108,62} M. L. PLANAS,⁹² W. PLASTINO,^{271,272} R. POGGIANI,^{80,19} E. POLINI,²⁷ L. POMPILI,¹
S. PONRATHNAM,^{14,†} J. POON,¹³⁹ E. PORCELLI,³² J. PORTELLI,^{38,73,245} E. K. PORTER,⁶³ C. POSNANSKY,⁸ R. POULTON,⁵⁴
J. POWELL,¹⁵⁵ M. PRACCHIA,²⁷ B. K. PRADHAN,¹⁴ T. PRADIER,¹⁷⁹ A. K. PRAJAPATI,⁸⁶ K. PRASAI,¹⁷ R. PRASANNA,²¹⁵
P. PRASIA,¹⁴ G. PRATTEN,¹¹⁵ M. PRINCIPE,^{134,89,270,106} G. A. PRODI,^{273,103} L. PROKHOROV,¹¹⁵ P. PROSPITO,^{132,133}
L. PRUDENZI,¹ A. PUECHER,^{32,68} J. PULLIN,¹⁰ M. PUNTURO,⁴⁷ F. PUOSI,^{19,80} P. PUPPO,⁶² M. PÜRERER,¹ H. QI,¹⁰ J. QIN,¹¹
V. QUETSCHKE,¹⁶³ P. J. QUINONEZ,⁴³ R. QUITZOW-JAMES,¹³⁶ F. J. RAAB,⁵² G. RAAIJMAKERS,^{97,32} N. RADULESCO,⁴⁴
P. RAFFAI,¹⁸⁹ S. X. RAIL,²³³ S. RAJA,⁹⁶ C. RAJAN,⁹⁶ K. E. RAMIREZ,⁶¹ A. RAMOS-BUADES,¹ D. RANA,¹⁴ E. RANDEL,¹³⁵
P. R. RANGNEKAR,¹⁷ P. RAPAGNANI,^{108,62} A. RAY,⁹ V. RAYMOND,¹⁸ N. RAZA,³⁰ M. RAZZANO,^{80,19} J. READ,⁵¹
M. RECAMAN PAYO,¹⁰¹ T. REGIMBAU,²⁷ L. REI,⁵³ S. REID,⁹¹ S. W. REID,¹¹⁴ D. H. REITZE,² P. RELTON,¹⁸ A. RENZINI,²
P. RETTEGNO,²⁴ B. REVENU,^{63,274} A. REZA,³² M. REZAC,⁵¹ A. S. REZAEI,^{62,108} F. RICCI,^{108,62} M. RICCI,⁶² D. RICHARDS,²⁰⁹
J. W. RICHARDSON,³⁴ A. RIJAL,⁴³ K. RILES,⁸² H. K. RILEY,¹⁸ S. RINALDI,^{80,19} C. ROBERTSON,²⁰⁹ N. A. ROBERTSON,²
F. ROBINET,³⁵ M. ROBINSON,⁵² A. ROCCHI,¹³³ L. ROLLAND,²⁷ J. G. ROLLINS,² M. ROMANELLI,¹⁰⁹ A. E. ROMANO,²⁷⁵
R. ROMANO,^{4,5} A. ROMERO,¹⁷⁶ I. M. ROMERO-SHAW,¹⁵ J. H. ROMIE,⁶¹ S. RONCHINI,^{40,111} T. J. ROOKE,⁹⁰ L. ROSA,^{5,28}
T. J. ROSAUER,³⁴ C. A. ROSE,⁹ D. ROSIŃSKA,¹¹⁶ M. P. ROSS,²⁰⁸ M. ROSSELLO,⁹² S. ROWAN,²⁵ S. ROY,⁶⁸ A. ROYZMAN,¹⁸⁸
D. ROZZA,^{168,130} P. RUGGI,⁵⁴ E. RUIZ MORALES,¹¹⁰ K. RUIZ-ROCHA,¹⁹² S. SACHDEV,⁵⁵ T. SADECKI,⁵² J. SADIQ,¹²³
P. SAFFARIEH,^{32,98} S. S. SAHA,¹⁴¹ T. SAINRAT,¹⁷⁹ S. SAJITH MENON,⁶² K. SAKAI,²⁷⁶ M. SAKELLARIADOU,⁶⁵ T. SAKO,¹⁵¹
S. SAKON,⁸ O. S. SALAFIA,^{118,119,157} F. SALCES-CARCOBA,² L. SALCONI,⁵⁴ M. SALEEM,²⁹ F. SALEMI,^{102,103} M. SALLÉ,³²
S. SALVADOR,^{197,196,259} A. SANCHEZ,⁵² E. J. SANCHEZ,² J. H. SANCHEZ,⁷² L. E. SANCHEZ,² N. SANCHIS-GUAL,^{277,137}
J. R. SANDERS,²⁷⁸ E. M. SÄNGER,¹ T. R. SARAVANAN,¹⁴ N. SARIN,⁷ A. SASLI,²¹³ P. SASSI,^{47,81} B. SASSOLAS,¹⁶⁷
H. SATARI,²⁶ R. SATO,²⁰⁶ S. SATO,¹⁵¹ Y. SATO,¹⁵¹ O. SAUTER,⁷⁸ R. L. SAVAGE,⁵² V. SAVANT,¹⁴ T. SAWADA,⁴⁵
H. L. SAWANT,¹⁴ S. SAYAH,¹⁶⁷ D. SCHAETZL,² M. SCHEEL,¹⁴⁹ S. J. SCHERF,¹⁷ J. SCHEUER,⁷² M. G. SCHIWORSKI,⁹⁰
P. SCHMIDT,¹¹⁵ S. SCHMIDT,⁶⁸ S. J. SCHMITZ,⁶⁷ R. SCHNABEL,⁷⁹ M. SCHNEEWIND,^{12,13} R. M. S. SCHOFIELD,⁶⁹
A. SCHÖNBECK,⁷⁹ K. SCHOUTEDEN,¹⁰¹ H. SCHULER,⁸ B. W. SCHULTE,^{12,13} B. F. SCHUTZ,^{18,1} E. SCHWARTZ,¹⁸ J. SCOTT,²⁵
S. M. SCOTT,¹¹ T. C. SEETHARAMU,²⁵ M. SEGLAR-ARROYO,³⁹ Y. SEKIGUCHI,²⁷⁹ D. SELLERS,⁶¹ A. S. SENGUPTA,²⁸⁰
D. SENTENAC,⁵⁴ E. G. SEO,²⁵ J. W. SEO,¹⁰¹ V. SEQUINO,^{28,5} G. SERVIGNAT,²⁶⁰ Y. SETYAWATI,⁶⁸ T. SHAFFER,⁵²
M. S. SHAHRIAR,⁷² M. A. SHAIKH,²²⁵ B. SHAMS,¹⁸⁸ L. SHAO,²¹² P. SHARMA,⁹⁶ S. SHARMA-CHAUDHARY,¹³⁶ P. SHAWHAN,¹¹⁷
N. S. SHCHEBLANOV,^{281,238} A. SHEELA,¹⁷² B. SHEN,¹¹⁷ K. G. SHEPARD,⁶⁴ Y. SHIKANO,^{282,283} M. SHIKAUCHI,¹²⁶
K. SHIMODE,⁴⁵ H. SHINKAI,²⁸⁴ J. SHIOTA,²⁵³ D. H. SHOEMAKER,⁷⁵ D. M. SHOEMAKER,¹⁴⁸ R. W. SHORT,⁵²
S. SHYAMSUNDAR,⁹⁶ A. SIDER,³³ H. SIEGEL,^{180,181} M. SIENIAWSKA,¹¹³ D. SIGG,⁵² L. SILENZI,^{47,48} M. SIMMONDS,⁹⁰
L. P. SINGER,⁷⁷ A. SINGH,¹⁹⁸ D. SINGH,⁸ M. K. SINGH,²⁰ A. SINGHA,^{31,32} A. M. SINTES,⁹² V. SIPALA,^{168,130} V. SKLIRIS,¹⁸
B. J. J. SLAGMOLEN,¹¹ T. J. SLAVEN-BLAIR,²⁶ J. SMETANA,¹¹⁵ J. R. SMITH,⁵¹ L. SMITH,²⁵ R. J. E. SMITH,⁷
J. SOLDATESCHI,^{239,285,60} S. N. SOMALA,²⁸⁶ K. SOMIYA,³ K. SONI,¹⁴ S. SONI,⁷⁵ V. SORDINI,¹⁵³ F. SORRENTINO,⁵³
N. SORRENTINO,^{80,19} R. SOULARD,⁴⁴ T. SOURADEEP,^{14,287} E. SOWELL,¹⁵⁹ V. SPAGNUOLO,^{31,32} A. P. SPENCER,²⁵
M. SPERA,^{83,84} P. SPINICELLI,⁵⁴ A. K. SRIVASTAVA,⁸⁶ V. SRIVASTAVA,⁷⁰ C. STACHIE,⁴⁴ F. STACHURSKI,²⁵ D. A. STEER,⁶³
J. STEINLECHNER,^{31,32} S. STEINLECHNER,^{31,32} D. STEPHENS,⁷² N. STERGIOLAS,²¹³ P. STEVENS,³⁵ M. STPIERRE,¹⁶²
L. C. STRANG,¹²⁹ G. STRATTA,^{288,289,62,290} M. D. STRONG,¹⁰ A. STRUNK,⁵² R. STURANI,²⁹¹ A. L. STUVER,⁹⁵
M. SUCHENEK,⁸⁸ S. SUDHAGAR,^{14,88} N. SUELTMANN,⁷⁹ H. G. SUH,⁹ A. G. SULLIVAN,¹⁶⁰ T. Z. SUMMERSCALES,⁶⁴ L. SUN,¹¹
S. SUNIL,⁸⁶ A. SUR,⁸⁸ J. SURESH,^{126,113} P. J. SUTTON,¹⁸ TAKAMASA SUZUKI,²⁰⁶ TAKANORI SUZUKI,³ B. L. SWINKELS,³²
A. SYX,¹⁷⁹ M. J. SZCZEPAŃCZYK,⁷⁸ P. SZEWCZYK,¹¹⁶ M. TACCA,³² H. TAGOSHI,¹⁵² S. C. TAIT,²⁵ H. TAKAHASHI,²⁹²
R. TAKAHASHI,²¹ A. TAKAMORI,⁵⁰ K. TAKATANI,¹⁹¹ H. TAKEDA,²⁹³ M. TAKEDA,¹⁹¹ C. J. TALBOT,⁹¹ C. TALBOT,⁷⁵
M. TAMAKI,¹⁵² N. TAMANINI,¹²⁰ D. TANABE,¹⁴³ K. TANAKA,¹⁵² S. J. TANAKA,²⁵³ T. TANAKA,²⁹³ A. J. TANASIJCZUK,¹¹³
S. TANIOKA,⁷⁰ D. B. TANNER,⁷⁸ D. TAO,² L. TAO,⁷⁸ R. D. TAPIA,⁸ E. N. TAPIA SAN MARTÍN,³² R. TARAFDER,²
C. TARANTO,¹³² A. TARUYA,²⁹⁴ J. D. TASSON,¹⁷³ M. TELOI,³³ R. TENORIO,⁹² L. TERKOWSKI,⁷⁹ H. THEMANN,¹⁹³
M. P. THIRUGNANASAMBANDAM,¹⁴ L. M. THOMAS,¹¹⁵ M. THOMAS,⁶¹ P. THOMAS,⁵² J. E. THOMPSON,¹⁸ S. R. THONDAPU,⁹⁶
K. A. THORNE,⁶¹ E. THRANE,⁷ J. TISSINO,⁴⁰ SHUBHANSHU TIWARI,¹⁷⁷ SRISHTI TIWARI,¹⁴ V. TIWARI,¹⁸ A. M. TOIVONEN,²⁹
A. E. TOLLEY,¹²¹ T. TOMARU,²¹ K. TOMITA,¹⁹¹ T. TOMURA,⁴⁵ M. TONELLI,^{80,19} A. TORIYAMA,²⁵³
A. TORRES-FORNÉ,^{137,138} C. I. TORRIE,² M. TOSCANI,¹²⁰ I. TOSTA E MELO,¹³⁰ E. TOURNEFIER,²⁷ A. A. TRANI,¹²⁶
A. TRAPANANTI,^{48,47} F. TRAVASSO,^{48,47} G. TRAYLOR,⁶¹ J. TRENADO,³⁸ M. TREVOR,¹¹⁷ M. C. TRINGALI,⁵⁴ A. TRIPATHEE,⁸²
L. TROIANO,^{295,106} A. TROVATO,^{42,248} L. TROZZO,⁵ R. J. TRUDEAU,² M. TSE,⁷⁵ R. TSO,¹⁴⁹ S. TSUCHIDA,²⁹⁶ L. TSUKADA,⁸
T. TSUTSUI,¹²⁶ K. TURBANG,^{176,107} M. TURCONI,⁴⁴ C. TURSKI,⁸⁷ H. UBACH,^{38,73} A. S. UBHI,¹¹⁵ N. UCHIKATA,¹⁵²
T. UCHIYAMA,⁴⁵ R. P. UDALL,² T. UEHARA,²⁹⁷ K. UENO,¹²⁶ C. S. UNNIKISHNAN,²⁵² T. USHIBA,⁴⁵ A. UTINA,^{31,32}
H. VAHLBRUCH,^{12,13} N. VAIDYA,² G. VAJENTE,² A. VAJPEYI,⁷ G. VALDES,¹²⁸ M. VALENTINI,^{98,32} S. A. VALLEJO-PEÑA,²⁷⁵
S. VALLERO,²⁴ V. VALSAL,⁹ N. VAN BAKEL,³² M. VAN BEUZEKOM,³² M. VAN DAEL,^{32,298} J. F. J. VAN DEN BRAND,^{31,98,32}
C. VAN DEN BROECK,^{68,32} D. C. VANDER-HYDE,⁷⁰ M. VAN DER SLUYS,^{32,68} A. VAN DE WALLE,³⁵ J. VAN DONGEN,^{32,98}
H. VAN HAEVERMAET,¹⁰⁷ J. V. VAN HELJNINGEN,¹¹³ J. VANOSKY,² M. H. P. M. VAN PUTTEN,²⁹⁹ Z. VAN RANST,^{31,32}
N. VAN REMORTEL,¹⁰⁷ M. VARDARO,^{31,32} A. F. VARGAS,¹²⁹ V. VARMA,¹ M. VASÚTH,⁷⁶ A. VECCHIO,¹¹⁵ G. VEDOVATO,⁸⁴
J. VEITCH,²⁵ P. J. VEITCH,⁹⁰ J. VENNEBERG,^{12,13} P. VERDIER,¹⁵³ D. VERKINDT,²⁷ P. VERMA,¹⁷⁴ Y. VERMA,⁹⁶
S. M. VERMEULEN,¹⁸ D. VESKE,¹⁶⁰ F. VETRANO,⁵⁹ A. VEUTRO,⁶² A. VICERÉ,^{59,60} S. VIDYANT,⁷⁰ A. D. VIETS,³⁰⁰
A. VIJAYKUMAR,²⁰ V. VILLA-ORTEGA,¹²³ E. T. VINCENT,⁵⁵ J.-Y. VINET,⁴⁴ S. VIRET,¹⁵³ A. VIRTUOSO,^{248,42} S. VITALE,⁷⁵
H. VOCCA,^{81,47} D. VOIGT,⁷⁹ E. R. G. VON REIS,⁵² J. S. A. VON WRANGEL,^{12,13} S. P. VYATCHANIN,⁹⁹ L. E. WADE,⁶⁷

M. WADE,⁶⁷ K. J. WAGNER,¹⁶¹ R. C. WALET,³² M. WALKER,¹¹⁴ G. S. WALLACE,⁹¹ L. WALLACE,² H. WANG,²⁶⁶
 J. Z. WANG,⁸² W. H. WANG,¹⁶³ R. L. WARD,¹¹ J. WARNER,⁵² M. WAS,²⁷ T. WASHIMI,²¹ N. Y. WASHINGTON,²
 K. WATADA,¹¹⁴ D. WATARAI,¹²⁶ K. E. WAYT,⁶⁷ B. WEAVER,⁵² C. R. WEAVING,¹²¹ S. A. WEBSTER,²⁵ M. WEINERT,^{12,13}
 A. J. WEINSTEIN,² R. WEISS,⁷⁵ C. M. WELLER,²⁰⁸ R. A. WELLER,¹⁹² F. WELLMANN,^{12,13} L. WEN,²⁶ P. WESSELS,^{12,13}
 K. WETTE,¹¹ J. T. WHELAN,¹⁶¹ D. D. WHITE,⁵¹ B. F. WHITING,⁷⁸ C. WHITTLE,⁷⁵ J. B. WILDBERGER,¹ O. S. WILK,⁶⁷
 D. WILKEN,^{12,13,13} K. WILLETTS,¹⁸ D. WILLIAMS,²⁵ M. J. WILLIAMS,²⁵ A. R. WILLIAMSON,¹²¹ J. L. WILLIS,²
 B. WILLKE,^{13,12,13} M. WILS,¹⁰¹ C. C. WIPF,² G. WOAN,²⁵ J. WOEHLENER,^{12,13} J. K. WOFFORD,¹⁶¹ D. WONG,³⁰
 H. T. WONG,¹⁴³ I. C. F. WONG,¹³⁹ M. WRIGHT,²⁵ C. WU,¹⁴¹ D. S. WU,^{12,13} H. WU,¹⁴¹ D. M. WYSOCKI,⁹ L. XIAO,²
 V. A. XU,⁷⁵ N. YADAV,⁸⁸ H. YAMAMOTO,² K. YAMAMOTO,¹⁵¹ M. YAMAMOTO,¹⁵¹ T. S. YAMAMOTO,²³² T. YAMAMOTO,⁴⁵
 S. YAMAMURA,¹⁵² R. YAMAZAKI,²⁵³ S. YAN,¹⁷ F. W. YANG,¹⁸⁸ K. Z. YANG,²⁹ L.-C. YANG,¹⁴⁶ Y.-C. YANG,¹⁴¹
 YANG YANG,⁷⁸ YI YANG,¹⁴⁶ M. J. YAP,¹¹ Z. YARBROUGH,¹⁰ S.-W. YEH,¹⁴¹ A. B. YELIKAR,¹⁶¹ S. M. C. YEUNG,⁹
 T. Y. YEUNG,⁶⁴ J. YOKOYAMA,^{36,37} T. YOKOZAWA,⁴⁵ J. YOO,³⁰¹ H. YU,¹⁴⁹ H. YUZURIHARA,⁴⁵ A. ZADROŻNY,¹⁷⁴
 A. J. ZANNELLI,¹¹⁴ M. ZANOLIN,⁴³ M. ZEESHAN,¹⁶¹ T. ZELENKOVA,⁵⁴ J.-P. ZENDRI,⁸⁴ M. ZEVIN,¹²⁴ J. ZHANG,¹¹ L. ZHANG,²
 R. ZHANG,⁷⁸ T. ZHANG,³⁰² YANQI ZHANG,¹²⁸ YA ZHANG,¹¹ C. ZHAO,²⁶ YUE ZHAO,¹⁸⁸ YUHANG ZHAO,^{152,21,63} Y. ZHENG,¹³⁶
 H. ZHONG,²⁹ R. ZHOU,²⁰³ Z.-H. ZHU,^{127,303} A. B. ZIMMERMAN,¹⁴⁸ M. E. ZUCKER,^{75,2} AND J. ZWEIZIG²
 THE LIGO SCIENTIFIC COLLABORATION, THE VIRGO COLLABORATION, AND THE KAGRA COLLABORATION

¹Max Planck Institute for Gravitational Physics (Albert Einstein Institute), D-14476 Potsdam, Germany

²LIGO Laboratory, California Institute of Technology, Pasadena, CA 91125, USA

³Graduate School of Science, Tokyo Institute of Technology, 2-12-1 Ookayama, Meguro-ku, Tokyo 152-8551, Japan

⁴Dipartimento di Farmacia, Università di Salerno, I-84084 Fisciano, Salerno, Italy

⁵INFN, Sezione di Napoli, I-80126 Napoli, Italy

⁶University of Warwick, Coventry CV4 7AL, United Kingdom

⁷OzGrav, School of Physics & Astronomy, Monash University, Clayton 3800, Victoria, Australia

⁸The Pennsylvania State University, University Park, PA 16802, USA

⁹University of Wisconsin-Milwaukee, Milwaukee, WI 53201, USA

¹⁰Louisiana State University, Baton Rouge, LA 70803, USA

¹¹OzGrav, Australian National University, Canberra, Australian Capital Territory 0200, Australia

¹²Max Planck Institute for Gravitational Physics (Albert Einstein Institute), D-30167 Hannover, Germany

¹³Leibniz Universität Hannover, D-30167 Hannover, Germany

¹⁴Inter-University Centre for Astronomy and Astrophysics, Pune 411007, India

¹⁵University of Cambridge, Cambridge CB2 1TN, United Kingdom

¹⁶Instituto Nacional de Pesquisas Espaciais, 12227-010 São José dos Campos, São Paulo, Brazil

¹⁷Stanford University, Stanford, CA 94305, USA

¹⁸Cardiff University, Cardiff CF24 3AA, United Kingdom

¹⁹INFN, Sezione di Pisa, I-56127 Pisa, Italy

²⁰International Centre for Theoretical Sciences, Tata Institute of Fundamental Research, Bengaluru 560089, India

²¹Gravitational Wave Science Project, National Astronomical Observatory of Japan, 2-21-1 Osawa, Mitaka City, Tokyo 181-8588, Japan

²²Advanced Technology Center, National Astronomical Observatory of Japan, 2-21-1 Osawa, Mitaka City, Tokyo 181-8588, Japan

²³Dipartimento di Fisica, Università degli Studi di Torino, I-10125 Torino, Italy

²⁴INFN Sezione di Torino, I-10125 Torino, Italy

²⁵SUPA, University of Glasgow, Glasgow G12 8QQ, United Kingdom

²⁶OzGrav, University of Western Australia, Crawley, Western Australia 6009, Australia

²⁷Univ. Savoie Mont Blanc, CNRS, Laboratoire d'Annecy de Physique des Particules - IN2P3, F-74000 Annecy, France

²⁸Università di Napoli "Federico II", I-80126 Napoli, Italy

²⁹University of Minnesota, Minneapolis, MN 55455, USA

³⁰University of British Columbia, Vancouver, BC V6T 1Z4, Canada

³¹Maastricht University, 6200 MD Maastricht, Netherlands

³²Nikhef, 1098 XG Amsterdam, Netherlands

³³Université Libre de Bruxelles, Brussels 1050, Belgium

³⁴University of California, Riverside, Riverside, CA 92521, USA

³⁵Université Paris-Saclay, CNRS/IN2P3, IJCLab, 91405 Orsay, France

³⁶Department of Physics, University of Tokyo, Bunkyo-ku, Tokyo 113-0033, Japan.

³⁷Research Center for the Early Universe (RESCEU), University of Tokyo, Bunkyo-ku, Tokyo 113-0033, Japan.

³⁸Institut de Ciències del Cosmos (ICCUB), Universitat de Barcelona (UB), c. Martí i Franquès, 1, 08028 Barcelona, Spain

³⁹Institut de Física d'Altes Energies (IFAE), The Barcelona Institute of Science and Technology, Campus UAB, E-08193 Bellaterra (Barcelona), Spain

⁴⁰Gran Sasso Science Institute (GSSI), I-67100 L'Aquila, Italy

- ⁴¹ *Dipartimento di Scienze Matematiche, Informatiche e Fisiche, Università di Udine, I-33100 Udine, Italy*
- ⁴² *INFN, Sezione di Trieste, I-34127 Trieste, Italy*
- ⁴³ *Embry-Riddle Aeronautical University, Prescott, AZ 86301, USA*
- ⁴⁴ *Université Côte d'Azur, Observatoire Côte d'Azur, CNRS, Artemis, F-06304 Nice, France*
- ⁴⁵ *Institute for Cosmic Ray Research, KAGRA Observatory, The University of Tokyo, 238 Higashi-Mozumi, Kamioka-cho, Hida City, Gifu 506-1205, Japan*
- ⁴⁶ *Department of Physics, National and Kapodistrian University of Athens, 15771 Ilissia, Greece*
- ⁴⁷ *INFN, Sezione di Perugia, I-06123 Perugia, Italy*
- ⁴⁸ *Università di Camerino, I-62032 Camerino, Italy*
- ⁴⁹ *American University, Washington, DC 20016, USA*
- ⁵⁰ *Earthquake Research Institute, The University of Tokyo, 1-1-1 Yayoi, Bunkyo-ku, Tokyo 113-0032, Japan*
- ⁵¹ *California State University Fullerton, Fullerton, CA 92831, USA*
- ⁵² *LIGO Hanford Observatory, Richland, WA 99352, USA*
- ⁵³ *INFN, Sezione di Genova, I-16146 Genova, Italy*
- ⁵⁴ *European Gravitational Observatory (EGO), I-56021 Cascina, Pisa, Italy*
- ⁵⁵ *Georgia Institute of Technology, Atlanta, GA 30332, USA*
- ⁵⁶ *Chennai Mathematical Institute, Chennai 603103, India*
- ⁵⁷ *Royal Holloway, University of London, London TW20 0EX, United Kingdom*
- ⁵⁸ *The Graduate University for Advanced Studies (SOKENDAI), 2-21-1 Osawa, Mitaka City, Tokyo 181-8588, Japan*
- ⁵⁹ *Università degli Studi di Urbino "Carlo Bo", I-61029 Urbino, Italy*
- ⁶⁰ *INFN, Sezione di Firenze, I-50019 Sesto Fiorentino, Firenze, Italy*
- ⁶¹ *LIGO Livingston Observatory, Livingston, LA 70754, USA*
- ⁶² *INFN, Sezione di Roma, I-00185 Roma, Italy*
- ⁶³ *Université Paris Cité, CNRS, Astroparticule et Cosmologie, F-75013 Paris, France*
- ⁶⁴ *Andrews University, Berrien Springs, MI 49104, USA*
- ⁶⁵ *King's College London, University of London, London WC2R 2LS, United Kingdom*
- ⁶⁶ *Korea Institute of Science and Technology Information, Daejeon 34141, Republic of Korea*
- ⁶⁷ *Kenyon College, Gambier, OH 43022, USA*
- ⁶⁸ *Institute for Gravitational and Subatomic Physics (GRASP), Utrecht University, 3584 CC Utrecht, Netherlands*
- ⁶⁹ *University of Oregon, Eugene, OR 97403, USA*
- ⁷⁰ *Syracuse University, Syracuse, NY 13244, USA*
- ⁷¹ *Université de Liège, B-4000 Liège, Belgium*
- ⁷² *Northwestern University, Evanston, IL 60208, USA*
- ⁷³ *Departament de Física Quàntica i Astrofísica (FQA), Universitat de Barcelona (UB), c. Martí i Franqués, 1, 08028 Barcelona, Spain*
- ⁷⁴ *Dipartimento di Medicina, Chirurgia e Odontoiatria "Scuola Medica Salernitana", Università di Salerno, I-84081 Baronissi, Salerno, Italy*
- ⁷⁵ *LIGO Laboratory, Massachusetts Institute of Technology, Cambridge, MA 02139, USA*
- ⁷⁶ *Wigner RCP, RMKI, H-1121 Budapest, Hungary*
- ⁷⁷ *NASA Goddard Space Flight Center, Greenbelt, MD 20771, USA*
- ⁷⁸ *University of Florida, Gainesville, FL 32611, USA*
- ⁷⁹ *Universität Hamburg, D-22761 Hamburg, Germany*
- ⁸⁰ *Università di Pisa, I-56127 Pisa, Italy*
- ⁸¹ *Università di Perugia, I-06123 Perugia, Italy*
- ⁸² *University of Michigan, Ann Arbor, MI 48109, USA*
- ⁸³ *Università di Padova, Dipartimento di Fisica e Astronomia, I-35131 Padova, Italy*
- ⁸⁴ *INFN, Sezione di Padova, I-35131 Padova, Italy*
- ⁸⁵ *Montana State University, Bozeman, MT 59717, USA*
- ⁸⁶ *Institute for Plasma Research, Bhat, Gandhinagar 382428, India*
- ⁸⁷ *Universiteit Gent, B-9000 Gent, Belgium*
- ⁸⁸ *Nicolaus Copernicus Astronomical Center, Polish Academy of Sciences, 00-716, Warsaw, Poland*
- ⁸⁹ *Dipartimento di Ingegneria, Università del Sannio, I-82100 Benevento, Italy*
- ⁹⁰ *OzGrav, University of Adelaide, Adelaide, South Australia 5005, Australia*
- ⁹¹ *SUPA, University of Strathclyde, Glasgow G1 1XQ, United Kingdom*
- ⁹² *IAC3-IIEEC, Universitat de les Illes Balears, E-07122 Palma de Mallorca, Spain*
- ⁹³ *Departament de Matemàtiques, Universitat Autònoma de Barcelona, 08193 Bellaterra (Barcelona), Spain*
- ⁹⁴ *Theoretisch-Physikalisches Institut, Friedrich-Schiller-Universität Jena, D-07743 Jena, Germany*
- ⁹⁵ *Villanova University, Villanova, PA 19085, USA*

- ⁹⁶RRCAT, Indore, Madhya Pradesh 452013, India
- ⁹⁷GRAPPA, Anton Pannekoek Institute for Astronomy and Institute for High-Energy Physics, University of Amsterdam, 1098 XH Amsterdam, Netherlands
- ⁹⁸Department of Physics and Astronomy, Vrije Universiteit Amsterdam, 1081 HV Amsterdam, Netherlands
- ⁹⁹Lomonosov Moscow State University, Moscow 119991, Russia
- ¹⁰⁰Center for Theoretical Physics, Polish Academy of Sciences, 02-668, Warsaw, Poland
- ¹⁰¹Katholieke Universiteit Leuven, Oude Markt 13, 3000 Leuven, Belgium
- ¹⁰²Università di Trento, Dipartimento di Fisica, I-38123 Povo, Trento, Italy
- ¹⁰³INFN, Trento Institute for Fundamental Physics and Applications, I-38123 Povo, Trento, Italy
- ¹⁰⁴Bar-Ilan University, Ramat Gan, 5290002, Israel
- ¹⁰⁵Dipartimento di Fisica "E.R. Caianiello", Università di Salerno, I-84084 Fisciano, Salerno, Italy
- ¹⁰⁶INFN, Sezione di Napoli, Gruppo Collegato di Salerno, I-80126 Napoli, Italy
- ¹⁰⁷Universiteit Antwerpen, 2000 Antwerpen, Belgium
- ¹⁰⁸Università di Roma "La Sapienza", I-00185 Roma, Italy
- ¹⁰⁹Univ Rennes, CNRS, Institut FOTON - UMR 6082, F-35000 Rennes, France
- ¹¹⁰Instituto de Fisica Teorica UAM-CSIC, Universidad Autonoma de Madrid, 28049 Madrid, Spain
- ¹¹¹INFN, Laboratori Nazionali del Gran Sasso, I-67100 Assergi, Italy
- ¹¹²Laboratoire Kastler Brossel, Sorbonne Université, CNRS, ENS-Université PSL, Collège de France, F-75005 Paris, France
- ¹¹³Université catholique de Louvain, B-1348 Louvain-la-Neuve, Belgium
- ¹¹⁴Christopher Newport University, Newport News, VA 23606, USA
- ¹¹⁵University of Birmingham, Birmingham B15 2TT, United Kingdom
- ¹¹⁶Astronomical Observatory Warsaw University, 00-478 Warsaw, Poland
- ¹¹⁷University of Maryland, College Park, MD 20742, USA
- ¹¹⁸Università degli Studi di Milano-Bicocca, I-20126 Milano, Italy
- ¹¹⁹INFN, Sezione di Milano-Bicocca, I-20126 Milano, Italy
- ¹²⁰L2IT, Laboratoire des 2 Infinis - Toulouse, Université de Toulouse, CNRS/IN2P3, UPS, F-31062 Toulouse Cedex 9, France
- ¹²¹University of Portsmouth, Portsmouth, PO1 3FX, United Kingdom
- ¹²²Université de Lyon, Université Claude Bernard Lyon 1, CNRS, Institut Lumière Matière, F-69622 Villeurbanne, France
- ¹²³IGFAE, Universidad de Santiago de Compostela, 15782 Spain
- ¹²⁴University of Chicago, Chicago, IL 60637, USA
- ¹²⁵Dipartimento di Fisica, Università degli Studi di Genova, I-16146 Genova, Italy
- ¹²⁶University of Tokyo, Tokyo, 113-0033, Japan.
- ¹²⁷Department of Astronomy, Beijing Normal University, Xijiekouwai Street 19, Haidian District, Beijing 100875, China
- ¹²⁸Texas A&M University, College Station, TX 77843, USA
- ¹²⁹OzGrav, University of Melbourne, Parkville, Victoria 3010, Australia
- ¹³⁰INFN, Laboratori Nazionali del Sud, I-95125 Catania, Italy
- ¹³¹Niels Bohr Institute, Copenhagen University, 2100 København, Denmark
- ¹³²Università di Roma Tor Vergata, I-00133 Roma, Italy
- ¹³³INFN, Sezione di Roma Tor Vergata, I-00133 Roma, Italy
- ¹³⁴University of Sannio at Benevento, I-82100 Benevento, Italy and INFN, Sezione di Napoli, I-80100 Napoli, Italy
- ¹³⁵Colorado State University, Fort Collins, CO 80523, USA
- ¹³⁶Missouri University of Science and Technology, Rolla, MO 65409, USA
- ¹³⁷Departamento de Astronomía y Astrofísica, Universitat de València, E-46100 Burjassot, València, Spain
- ¹³⁸Observatori Astronòmic, Universitat de València, E-46980 Paterna, València, Spain
- ¹³⁹The Chinese University of Hong Kong, Shatin, NT, Hong Kong
- ¹⁴⁰Indian Institute of Technology Bombay, Powai, Mumbai 400 076, India
- ¹⁴¹National Tsing Hua University, Hsinchu City 30013, Taiwan
- ¹⁴²Department of Physics, National Cheng Kung University, No.1, University Road, Tainan City 701, Taiwan
- ¹⁴³National Central University, Taoyuan City 320317, Taiwan
- ¹⁴⁴OzGrav, Charles Sturt University, Wagga Wagga, New South Wales 2678, Australia
- ¹⁴⁵Queen Mary University of London, London E1 4NS, United Kingdom
- ¹⁴⁶Department of Electrophysics, National Yang Ming Chiao Tung University, 101 Univ. Street, Hsinchu, Taiwan
- ¹⁴⁷Kamioka Branch, National Astronomical Observatory of Japan, 238 Higashi-Mozumi, Kamioka-cho, Hida City, Gifu 506-1205, Japan
- ¹⁴⁸University of Texas, Austin, TX 78712, USA
- ¹⁴⁹CaRT, California Institute of Technology, Pasadena, CA 91125, USA
- ¹⁵⁰Dipartimento di Ingegneria Industriale (DIIN), Università di Salerno, I-84084 Fisciano, Salerno, Italy
- ¹⁵¹Faculty of Science, University of Toyama, 3190 Gofuku, Toyama City, Toyama 930-8555, Japan

- ¹⁵²*Institute for Cosmic Ray Research, KAGRA Observatory, The University of Tokyo, 5-1-5 Kashiwa-no-Ha, Kashiwa City, Chiba 277-8582, Japan*
- ¹⁵³*Université Lyon, Université Claude Bernard Lyon 1, CNRS, IP2I Lyon / IN2P3, UMR 5822, F-69622 Villeurbanne, France*
- ¹⁵⁴*INAF, Osservatorio Astronomico di Padova, I-35122 Padova, Italy*
- ¹⁵⁵*OzGrav, Swinburne University of Technology, Hawthorn VIC 3122, Australia*
- ¹⁵⁶*Université libre de Bruxelles, 1050 Bruxelles, Belgium*
- ¹⁵⁷*INAF, Osservatorio Astronomico di Brera sede di Merate, I-23807 Merate, Lecco, Italy*
- ¹⁵⁸*Departamento de Matemáticas, Universitat de València, E-46100 Burjassot, València, Spain*
- ¹⁵⁹*Texas Tech University, Lubbock, TX 79409, USA*
- ¹⁶⁰*Columbia University, New York, NY 10027, USA*
- ¹⁶¹*Rochester Institute of Technology, Rochester, NY 14623, USA*
- ¹⁶²*University of Rhode Island, Kingston, RI 02881, USA*
- ¹⁶³*The University of Texas Rio Grande Valley, Brownsville, TX 78520, USA*
- ¹⁶⁴*Bellevue College, Bellevue, WA 98007, USA*
- ¹⁶⁵*Scuola Normale Superiore, I-56126 Pisa, Italy*
- ¹⁶⁶*The University of Sheffield, Sheffield S10 2TN, United Kingdom*
- ¹⁶⁷*Université Lyon, Université Claude Bernard Lyon 1, CNRS, Laboratoire des Matériaux Avancés (LMA), IP2I Lyon / IN2P3, UMR 5822, F-69622 Villeurbanne, France*
- ¹⁶⁸*Università degli Studi di Sassari, I-07100 Sassari, Italy*
- ¹⁶⁹*Dipartimento di Scienze Matematiche, Fisiche e Informatiche, Università di Parma, I-43124 Parma, Italy*
- ¹⁷⁰*INFN, Sezione di Milano Bicocca, Gruppo Collegato di Parma, I-43124 Parma, Italy*
- ¹⁷¹*Corps des Mines, Mines Paris, Université PSL, 60 Bd Saint-Michel, 75272 Paris, France*
- ¹⁷²*Indian Institute of Technology Madras, Chennai 600036, India*
- ¹⁷³*Carleton College, Northfield, MN 55057, USA*
- ¹⁷⁴*National Center for Nuclear Research, 05-400 Świerk-Otwock, Poland*
- ¹⁷⁵*Institut d'Astrophysique de Paris, Sorbonne Université, CNRS, UMR 7095, 75014 Paris, France*
- ¹⁷⁶*Vrije Universiteit Brussel, 1050 Brussel, Belgium*
- ¹⁷⁷*University of Zurich, Winterthurerstrasse 190, 8057 Zurich, Switzerland*
- ¹⁷⁸*Canadian Institute for Theoretical Astrophysics, University of Toronto, Toronto, ON M5S 3H8, Canada*
- ¹⁷⁹*Université de Strasbourg, CNRS, IPHC UMR 7178, F-67000 Strasbourg, France*
- ¹⁸⁰*Stony Brook University, Stony Brook, NY 11794, USA*
- ¹⁸¹*Center for Computational Astrophysics, Flatiron Institute, New York, NY 10010, USA*
- ¹⁸²*Montclair State University, Montclair, NJ 07043, USA*
- ¹⁸³*Institute for Nuclear Research, H-4026 Debrecen, Hungary*
- ¹⁸⁴*CNR-SPIN, I-84084 Fisciano, Salerno, Italy*
- ¹⁸⁵*Scuola di Ingegneria, Università della Basilicata, I-85100 Potenza, Italy*
- ¹⁸⁶*Western Washington University, Bellingham, WA 98225, USA*
- ¹⁸⁷*SUPA, University of the West of Scotland, Paisley PA1 2BE, United Kingdom*
- ¹⁸⁸*The University of Utah, Salt Lake City, UT 84112, USA*
- ¹⁸⁹*Eötvös University, Budapest 1117, Hungary*
- ¹⁹⁰*Centro de Física das Universidades do Minho e do Porto, Universidade do Minho, PT-4710-057 Braga, Portugal*
- ¹⁹¹*Department of Physics, Graduate School of Science, Osaka Metropolitan University, 3-3-138 Sugimoto-cho, Sumiyoshi-ku, Osaka City, Osaka 558-8585, Japan*
- ¹⁹²*Vanderbilt University, Nashville, TN 37235, USA*
- ¹⁹³*California State University, Los Angeles, Los Angeles, CA 90032, USA*
- ¹⁹⁴*University of Szeged, Dóm tér 9, Szeged 6720, Hungary*
- ¹⁹⁵*INAF, Osservatorio Astronomico di Capodimonte, I-80131 Napoli, Italy*
- ¹⁹⁶*Université de Normandie, ENSICAEN, UNICAEN, CNRS/IN2P3, LPC Caen, F-14000 Caen, France*
- ¹⁹⁷*Laboratoire de Physique Corpusculaire Caen, 6 boulevard du maréchal Juin, F-14050 Caen, France*
- ¹⁹⁸*The University of Mississippi, University, MS 38677, USA*
- ¹⁹⁹*Institute of Physics, Academia Sinica, 128 Sec. 2, Academia Rd., Nankang, Taipei 11529, Taiwan*
- ²⁰⁰*Shanghai Astronomical Observatory, Chinese Academy of Sciences, 80 Nandan Road, Shanghai 200030, China*
- ²⁰¹*University of Nevada, Las Vegas, Las Vegas, NV 89154, USA*
- ²⁰²*Department of Applied Physics, Fukuoka University, 8-19-1 Nanakuma, Jonan, Fukuoka City, Fukuoka 814-0180, Japan*
- ²⁰³*University of California, Berkeley, CA 94720, USA*
- ²⁰⁴*University of Lancaster, Lancaster LA1 4YW, United Kingdom*
- ²⁰⁵*College of Industrial Technology, Nihon University, 1-2-1 Izumi, Narashino City, Chiba 275-8575, Japan*

- ²⁰⁶ Faculty of Engineering, Niigata University, 8050 Ikarashi-2-no-cho, Nishi-ku, Niigata City, Niigata 950-2181, Japan
- ²⁰⁷ Department of Physics, Tamkang University, No. 151, Yingzhuang Rd., Danshui Dist., New Taipei City 25137, Taiwan
- ²⁰⁸ University of Washington, Seattle, WA 98195, USA
- ²⁰⁹ Rutherford Appleton Laboratory, Didcot OX11 0DE, United Kingdom
- ²¹⁰ Department of Astronomy and Space Science, Chungnam National University, 9 Daehak-ro, Yuseong-gu, Daejeon 34134, Republic of Korea
- ²¹¹ Institute of Applied Physics, Nizhny Novgorod, 603950, Russia
- ²¹² Kavli Institute for Astronomy and Astrophysics, Peking University, Yiheyuan Road 5, Haidian District, Beijing 100871, China
- ²¹³ Department of Physics, Aristotle University of Thessaloniki, 54124 Thessaloniki, Greece
- ²¹⁴ Nambu Yoichiro Institute of Theoretical and Experimental Physics (NITEP), Osaka Metropolitan University, 3-3-138 Sugimoto-cho, Sumiyoshi-ku, Osaka City, Osaka 558-8585, Japan
- ²¹⁵ Directorate of Construction, Services & Estate Management, Mumbai 400094, India
- ²¹⁶ University of Białystok, 15-424 Białystok, Poland
- ²¹⁷ National Astronomical Observatories, Chinese Academic of Sciences, 20A Datun Road, Chaoyang District, Beijing, China
- ²¹⁸ School of Astronomy and Space Science, University of Chinese Academy of Sciences, 20A Datun Road, Chaoyang District, Beijing, China
- ²¹⁹ University of Southampton, Southampton SO17 1BJ, United Kingdom
- ²²⁰ Department of Physics, Ulsan National Institute of Science and Technology (UNIST), 50 UNIST-gil, Ulju-gun, Ulsan 44919, Republic of Korea
- ²²¹ Institute for High-Energy Physics, University of Amsterdam, 1098 XH Amsterdam, Netherlands
- ²²² Chung-Ang University, Seoul 06974, Republic of Korea
- ²²³ University of Washington Bothell, Bothell, WA 98011, USA
- ²²⁴ Ewha Womans University, Seoul 03760, Republic of Korea
- ²²⁵ Seoul National University, Seoul 08826, Republic of Korea
- ²²⁶ Sungkyunkwan University, Seoul 03063, Republic of Korea
- ²²⁷ National Institute for Mathematical Sciences, Daejeon 34047, Republic of Korea
- ²²⁸ Ulsan National Institute of Science and Technology, Ulsan 44919, Republic of Korea
- ²²⁹ Institute of Particle and Nuclear Studies (IPNS), High Energy Accelerator Research Organization (KEK), 1-1 Oho, Tsukuba City, Ibaraki 305-0801, Japan
- ²³⁰ Bard College, Annandale-On-Hudson, NY 12504, USA
- ²³¹ Institute of Mathematics, Polish Academy of Sciences, 00656 Warsaw, Poland
- ²³² Department of Physics, Nagoya University, ES building, Furocho, Chikusa-ku, Nagoya, Aichi 464-8602, Japan
- ²³³ Université de Montréal/Polytechnique, Montreal, Quebec H3T 1J4, Canada
- ²³⁴ Université Côte d'Azur, Observatoire Côte d'Azur, CNRS, Lagrange, F-06304 Nice, France
- ²³⁵ Inje University Gimhae, South Gyeongsang 50834, Republic of Korea
- ²³⁶ Technology Center for Astronomy and Space Science, Korea Astronomy and Space Science Institute (KASI), 776 Daedeokdae-ro, Yuseong-gu, Daejeon 34055, Republic of Korea
- ²³⁷ Perimeter Institute, Waterloo, ON N2L 2Y5, Canada
- ²³⁸ NAVIER, École des Ponts, Univ Gustave Eiffel, CNRS, Marne-la-Vallée, France
- ²³⁹ Università di Firenze, Sesto Fiorentino I-50019, Italy
- ²⁴⁰ Department of Physics, University of Trento, via Sommarive 14, Povo, 38123 TN, Italy
- ²⁴¹ National Center for High-performance computing, National Applied Research Laboratories, No. 7, R&D 6th Rd., Hsinchu Science Park, Hsinchu City 30076, Taiwan
- ²⁴² NASA Marshall Space Flight Center, Huntsville, AL 35811, USA
- ²⁴³ West Virginia University, Morgantown, WV 26506, USA
- ²⁴⁴ School of Physics Science and Engineering, Tongji University, Shanghai 200092, China
- ²⁴⁵ Institut d'Estudis Espacials de Catalunya, c. Gran Capità, 2-4, 08034 Barcelona, Spain
- ²⁴⁶ Institució Catalana de Recerca i Estudis Avançats (ICREA), Passeig de Lluís Companys, 23, 08010 Barcelona, Spain
- ²⁴⁷ Tsinghua University, Beijing 100084, China
- ²⁴⁸ Dipartimento di Fisica, Università di Trieste, I-34127 Trieste, Italy
- ²⁴⁹ Institute for Photon Science and Technology, The University of Tokyo, 2-11-16 Yayoi, Bunkyo-ku, Tokyo 113-8656, Japan
- ²⁵⁰ INFN Cagliari, Physics Department, Università degli Studi di Cagliari, Cagliari 09042, Italy
- ²⁵¹ Saha Institute of Nuclear Physics, Bidhannagar, West Bengal 700064, India
- ²⁵² Tata Institute of Fundamental Research, Mumbai 400005, India
- ²⁵³ Department of Physical Sciences, Aoyama Gakuin University, 5-10-1 Fuchinobe, Sagami-hara City, Kanagawa 252-5258, Japan
- ²⁵⁴ Institut des Hautes Etudes Scientifiques, F-91440 Bures-sur-Yvette, France
- ²⁵⁵ Faculty of Law, Ryukoku University, 67 Fukakusa Tsukamoto-cho, Fushimi-ku, Kyoto City, Kyoto 612-8577, Japan
- ²⁵⁶ Indian Institute of Science Education and Research, Kolkata, Mohanpur, West Bengal 741252, India

- ²⁵⁷ *Department of Physics and Astronomy, University of Notre Dame, 225 Nieuwland Science Hall, Notre Dame, IN 46556, USA*
- ²⁵⁸ *Department of Astronomy, The University of Tokyo, 7-3-1 Hongo, Bunkyo-ku, Tokyo 113-0033, Japan*
- ²⁵⁹ *Centre national de la recherche scientifique, 75016 Paris, France*
- ²⁶⁰ *Laboratoire Univers et Théories, Observatoire de Paris, 92190 Meudon, France*
- ²⁶¹ *Observatoire de Paris, 75014 Paris, France*
- ²⁶² *Université PSL, 75006 Paris, France*
- ²⁶³ *Université de Paris Cité, 75006 Paris, France*
- ²⁶⁴ *Graduate School of Science and Technology, Niigata University, 8050 Ikarashi-2-no-cho, Nishi-ku, Niigata City, Niigata 950-2181, Japan*
- ²⁶⁵ *Niigata Study Center, The Open University of Japan, 754 Ichibancho, Asahimachi-dori, Chuo-ku, Niigata City, Niigata 951-8122, Japan*
- ²⁶⁶ *Department of Physics, The University of Tokyo, 7-3-1 Hongo, Bunkyo-ku, Tokyo 113-0033, Japan*
- ²⁶⁷ *CSIR-Central Glass and Ceramic Research Institute, Kolkata, West Bengal 700032, India*
- ²⁶⁸ *Consiglio Nazionale delle Ricerche - Istituto dei Sistemi Complessi, I-00185 Roma, Italy*
- ²⁶⁹ *Hobart and William Smith Colleges, Geneva, NY 14456, USA*
- ²⁷⁰ *Museo Storico della Fisica e Centro Studi e Ricerche “Enrico Fermi”, I-00184 Roma, Italy*
- ²⁷¹ *Dipartimento di Ingegneria Industriale, Eletttronica e Meccanica, Università degli Studi Roma Tre, I-00146 Roma, Italy*
- ²⁷² *INFN, Sezione di Roma Tre, I-00146 Roma, Italy*
- ²⁷³ *Università di Trento, Dipartimento di Matematica, I-38123 Povo, Trento, Italy*
- ²⁷⁴ *Subatech, CNRS/IN2P3 - Institut Mines-Telecom Atlantique - Université de Nantes, 4 rue Alfred Kastler BP 20722 44307 Nantes C’EDEX 03, France*
- ²⁷⁵ *Universidad de Antioquia, Medellín, Colombia*
- ²⁷⁶ *Department of Electronic Control Engineering, National Institute of Technology, Nagaoka College, 888 Nishikatahai, Nagaoka City, Niigata 940-8532, Japan*
- ²⁷⁷ *Departamento de Matemática da Universidade de Aveiro and Centre for Research and Development in Mathematics and Applications, 3810-183 Aveiro, Portugal*
- ²⁷⁸ *Marquette University, Milwaukee, WI 53233, USA*
- ²⁷⁹ *Faculty of Science, Toho University, 2-2-1 Miyama, Funabashi City, Chiba 274-8510, Japan*
- ²⁸⁰ *Indian Institute of Technology, Palaj, Gandhinagar, Gujarat 382355, India*
- ²⁸¹ *Laboratoire MSME, Cité Descartes, 5 Boulevard Descartes, Champs-sur-Marne, 77454 Marne-la-Vallée Cedex 2, France*
- ²⁸² *Graduate School of Science and Technology, Gunma University, 4-2 Aramaki, Maebashi, Gunma 371-8510, Japan*
- ²⁸³ *Institute for Quantum Studies, Chapman University, 1 University Dr., Orange, CA 92866, USA*
- ²⁸⁴ *Faculty of Information Science and Technology, Osaka Institute of Technology, 1-79-1 Kitayama, Hirakata City, Osaka 573-0196, Japan*
- ²⁸⁵ *INAF, Osservatorio Astrofisico di Arcetri, I-50125 Firenze, Italy*
- ²⁸⁶ *Indian Institute of Technology Hyderabad, Sangareddy, Khandi, Telangana 502285, India*
- ²⁸⁷ *Indian Institute of Science Education and Research, Pune, Maharashtra 411008, India*
- ²⁸⁸ *Institut für Theoretische Physik, Johann Wolfgang Goethe-Universität, Max-von-Laue-Str. 1, 60438 Frankfurt am Main, Germany*
- ²⁸⁹ *Istituto di Astrofisica e Planetologia Spaziali di Roma, 00133 Roma, Italy*
- ²⁹⁰ *INAF, Osservatorio di Astrofisica e Scienza dello Spazio, I-40129 Bologna, Italy*
- ²⁹¹ *Universidade Estadual Paulista, 01140-070 Campinas, São Paulo, Brazil*
- ²⁹² *Research Center for Space Science, Advanced Research Laboratories, Tokyo City University, 8-15-1 Todoroki, Setagaya, Tokyo 158-0082, Japan*
- ²⁹³ *Department of Physics, Kyoto University, Kita-Shirakawa Oiwake-cho, Sakyou-ku, Kyoto City, Kyoto 606-8502, Japan*
- ²⁹⁴ *Yukawa Institute for Theoretical Physics (YITP), Kyoto University, Kita-Shirakawa Oiwake-cho, Sakyou-ku, Kyoto City, Kyoto 606-8502, Japan*
- ²⁹⁵ *Dipartimento di Scienze Aziendali - Management and Innovation Systems (DISA-MIS), Università di Salerno, I-84084 Fisciano, Salerno, Italy*
- ²⁹⁶ *National Institute of Technology, Fukui College, Geshi-cho, Sabae-shi, Fukui 916-8507, Japan*
- ²⁹⁷ *Department of Communications Engineering, National Defense Academy of Japan, 1-10-20 Hashirimizu, Yokosuka City, Kanagawa 239-8686, Japan*
- ²⁹⁸ *Eindhoven University of Technology, 5600 MB Eindhoven, Netherlands*
- ²⁹⁹ *Department of Physics and Astronomy, Sejong University, 209 Neungdong-ro, Gwangjin-gu, Seoul 143-747, Republic of Korea*
- ³⁰⁰ *Concordia University Wisconsin, Mequon, WI 53097, USA*
- ³⁰¹ *Cornell University, Ithaca, NY 14850, USA*
- ³⁰² *Maastricht University, 6200 MD, Maastricht, Netherlands*
- ³⁰³ *School of Physics and Technology, Wuhan University, Bayi Road 299, Wuchang District, Wuhan, Hubei, 430072, China*

ABSTRACT

Despite the growing number of confident binary black hole coalescences observed through gravitational waves so far, the astrophysical origin of these binaries remains uncertain. Orbital eccentricity is one of the clearest tracers of binary formation channels. Identifying binary eccentricity, however, remains challenging due to the limited availability of gravitational waveforms that include effects of eccentricity. Here, we present observational results for a waveform-independent search sensitive to eccentric black hole coalescences, covering the third observing run (O3) of the LIGO and Virgo detectors. We identified no new high-significance candidates beyond those that were already identified with searches focusing on quasi-circular binaries. We determine the sensitivity of our search to high-mass (total mass $M > 70 M_{\odot}$) binaries covering eccentricities up to 0.3 at 15 Hz orbital frequency, and use this to compare model predictions to search results. Assuming all detections are indeed quasi-circular, for our fiducial population model, we place an upper limit for the merger rate density of high-mass binaries with eccentricities $0 < e \leq 0.3$ at $0.33 \text{ Gpc}^{-3} \text{ yr}^{-1}$ at 90% confidence level.

Keywords: Gravitational wave sources, eccentricity, black holes

1. INTRODUCTION

The LIGO (Aasi et al. 2015) and Virgo (Acernese et al. 2015) gravitational wave observatories have completed three observing runs thus far. During these runs, 90 compact binary merger candidates were identified that had probability of astrophysical origin $p_{\text{astro}} > 0.5$ (Abbott et al. 2021b; Abbott et al. 2021a). These discoveries opened previously inaccessible avenues to study the Universe, including the first direct information on binary black holes (Abbott et al. 2016a,b), the multi-messenger observation of a binary neutron star coalescence (Abbott et al. 2017; Abbott et al. 2017a; Margutti & Chornock 2021), a new type of constraint on cosmic expansion (Abbott et al. 2017b; Abbott et al. 2021b), and novel tests of general relativity (Abbott et al. 2016c, 2017c; Abbott et al. 2021c).

Despite the growing number of candidates and the insight they have provided, the astrophysical sites and processes that produce the observed merging binaries remain uncertain. Multiple viable scenarios exist. The binary black holes could have formed in an isolated stellar binary (e.g., Bethe & Brown 1998; Dominik et al. 2015; Inayoshi et al. 2017; Marchant et al. 2016; de Mink & Mandel 2016; Gallegos-Garcia et al. 2021), via dynamical interactions in dense stellar clusters (e.g., Portegies Zwart & McMillan 2000; Banerjee et al. 2010; Ziosi et al. 2014; Morscher et al. 2015; Mapelli 2016; Rodriguez et al. 2016a; Askar et al. 2017) or triple systems (e.g., Antonini et al. 2017; Martinez et al. 2020; Vigna-Gómez et al. 2021), or via gas capture in the disks of active galactic nuclei (AGN; e.g., McKernan et al. 2012; Bartos et al. 2017; Fragione et al. 2019; Tagawa et al. 2020).

Gravitational waves carry information about the masses and spins of the merging black holes, which can be used to probe the binaries' origin (Abbott et al. 2016b; Vitale et al. 2017; Zevin et al. 2021). Different formation channels have diverse predictions for the most common component masses, mass ratios, spin magnitudes and spin orientations (Belczynski et al. 2002; Dominik et al. 2013; Vitale et al. 2017). For example, isolated binaries are typically expected to produce black holes with spins mostly aligned with the binary's orbital axis with possible misalignments that could stem from recoil velocities imparted during supernova explosion (e.g., Rodriguez et al. 2016b; Gerosa et al. 2018; Wysocki et al. 2019). Dynamically formed binaries, on the other hand, generally have an isotropic spin distribution (e.g., Rodriguez et al. 2016b; Fishbach et al. 2017; Baibhav et al. 2020). However, while masses and spins provide crucial information about the binaries' origin, there is often overlap between their distributions for various formation channels. A catalogue of binary black holes must therefore be considered to make statistical inferences about their origins using these properties alone.

Orbital eccentricity, e is a unique signature that disfavors isolated binaries and favors triple systems, stellar clusters or AGN-assisted mergers as the possible formation scenario of the binary. While isolated black hole binaries can be born with an initial eccentricity, gravitational-wave emission will circularize their orbit by the time their orbital frequency reaches the sensitive band of ground-based gravitational-wave observatories (Peters 1964). Dynamical encounters can form binaries closer to merger, leaving insufficient time for orbital circularization. In AGN disks, eccentricity can be enhanced for a significant fraction of mergers, e.g., via binary–single interactions (Samsing et al. 2022; Tagawa

* Deceased, November 2022.

† Deceased, March 2022.

et al. 2021). Eccentricity can also be enhanced for field binaries by a nearby third object via the Kozai–Lidov mechanism (Kozai 1962; Lidov 1962; Naoz 2016; Antonini et al. 2017; Randall & Xianyu 2018; Bartos et al. 2023). Identifying orbital eccentricity (or the lack thereof) in the population of binary black holes consequently places clear constraints on the proportion of binaries originating from various formation channels.

Despite the advantages that come with estimating the binary’s orbital eccentricity, it has been difficult to probe this parameter through gravitational-wave observations for several reasons. (i) Eccentric orbits have wider dynamical range than quasi-circular, or $e = 0$ orbits, making them more challenging to model semi-analytically (Huerta et al. 2014; Tanay et al. 2016). (ii) Eccentricity increases the dimension of the binary parameter space, requiring more gravitational waveform templates and substantially increasing the computational cost of both waveform computation (Cornish & Shapiro Key 2010) and running template-based searches (Lenon et al. 2021). (iii) Given these challenges and the lack of expected eccentricity in field binaries, the development of eccentric waveform models began with significant delay compared to circular waveform models (Junker & Schaefer 1992). Nonetheless, eccentric waveform development has been an active area recently, with several promising waveform models that can be useful in the future (e.g., Hinderer & Babak 2017; Cao & Han 2017; Liu et al. 2022; Nagar et al. 2021; Albanesi et al. 2021; Khalil et al. 2021; Ramos-Buades et al. 2022; Islam et al. 2021; Setyawati & Ohme 2021; Wang et al. 2023).

While no comprehensive eccentric gravitational-wave template bank is currently available, indications of eccentricity already exist within the catalog of detected gravitational waves. The basis of such results is that standard gravitational-wave search algorithms developed to target circular binaries also have some sensitivity to eccentric binaries. For low masses $\lesssim 10 M_{\odot}$, circular template-based searches show undiminished sensitivity for small residual eccentricities ($e \lesssim 0.05$ at 40 Hz). To detect signals with eccentricities beyond $e \gtrsim 0.1$, we would however require template banks that include eccentric waveforms (Brown & Zimmerman 2010). In contrast, for higher masses and eccentricities, it has been shown that eccentricities can be found without significant loss of signal-to-noise ratio (SNR) using model-agnostic searches (Abbott et al. 2019).

To identify detected binaries as eccentric, two approaches have been carried out so far that circumvent the need for comprehensive template banks:

- One approach is to employ Bayesian analyses using existing eccentric waveform models. An ec-

centric waveform model limited to eccentricities $e < 0.2$ was used to show that the binary merger that produced the signal GW190521 as well as two others are consistent with originating from eccentric binary black holes (eBBH). (Romero-Shaw et al. 2020, 2021). Using a different waveform model that includes the full eccentricity range, Gamba et al. (2023) found strong support for the binary coalescence that produced GW190521 being highly eccentric. Both models were limited to waveforms with black hole spins aligned with the binary orbit. Orbital eccentricity and misaligned spins that induce precession of the orbital plane produce similar imprints in the gravitational wave, and both of these effects should preferably be accounted for in order to accurately analyze the event (Calderón Bustillo et al. 2021; Romero-Shaw et al. 2023).

- A different approach relies on numerical relativity simulations of eBBHs. Due to the computational cost, only a limited number of simulations can be carried out, which can only sparsely cover the parameter space. Gayathri et al. (2022) used such numerical relativity waveforms that discretely cover the full eccentricity space and includes waveforms with both aligned and misaligned spin with the binary orbit. Interpolation methods and consistency checks were applied to recover the eccentricity and other parameters of the binary. They found that the signal GW190521 is most consistent with being produced by a highly eccentric ($e \sim 0.7$) binary.

The GW190521 signal for which the above analyses were applied was already considered special even without the indication of eccentricity, having had a high reconstructed total black hole mass of $153.1_{-16.2}^{+42.2} M_{\odot}$, along with high and probably misaligned spin (Abbott et al. 2020).

In this paper, we carry out a search focusing on eccentric black hole coalescences over the third observing run (O3) of the LIGO–Virgo network. We use a minimally modeled search algorithm (Klimenko et al. 2005; Salemi et al. 2019; Tiwari et al. 2016) that we optimize for sensitivity for a set of high-mass (total mass $M \geq 70 M_{\odot}$), eccentric gravitational waveforms (Hinder et al. 2018; Boyle et al. 2019). As methods to estimate the eccentricity of individual events are under development, we instead focus on potential detections that have not already been discovered by other searches, and characterize the sensitivity of our search to eccentric binaries, relying on methods with well understood performance.

The paper is organized as follows. In Section 2 we introduce our search algorithm and demonstrate its sensitivity to eccentric waveforms. In Section 3 we present our search results. In Section 4 we discuss constraints on astrophysical populations based on our search results. We conclude in Section 5.

Gravitational wave strain data (LIGO Scientific Collaboration, Virgo Collaboration and KAGRA Collaboration 2021) and posterior samples (Abbott et al. 2021a) for all events from GWTC-3 are available from the Zenodo platform or the Gravitational Wave Open Science Center (Abbott et al. 2021b).

2. SEARCH ALGORITHM AND SENSITIVITY

2.1. Characterization of eccentricity

Due to the emission of gravitational waves, binary orbits have a gradually decreasing orbital separation. Eccentric binary orbits also circularize over time due to the emission of gravitational waves (Peters 1964). This makes the definition of eccentricity challenging. Determining eccentricity is particularly difficult at the late stages of the binary evolution when less than a full orbit separates the black holes from merger.

There have been various efforts to define eccentricity for binary compact object systems. These eccentricity definitions involve Keplerian orbit assumptions (Peters & Mathews 1963; Loutrel et al. 2018), angular frequencies at apocenter and pericenter (Mora & Will 2004), calculations using instantaneous radial acceleration (Healy et al. 2018) and using coordinate separations (Buonanno et al. 2011). A detailed list of the different eccentricity definitions that have been developed so far can be found in Loutrel et al. (2018).

For our analysis, we adopt the eccentricity definition following Ramos-Buades et al. (2022), based on calculation first developed by Mora & Will (2004) and later used by Lewis et al. (2017), Ramos-Buades et al. (2020) and Shaikh et al. (2023). To compute eccentricity for each orbit, we used the gravitational-wave frequencies at apocenter (ω_a) and the consecutive pericenter (ω_p). With these, eccentricity for the given orbit is

$$e = \cos(\psi/3) - \sqrt{3} \sin(\psi/3) \quad (1)$$

with

$$\psi = \arctan\left(\frac{1 - e_{22}^2}{2e_{22}}\right), \quad (2)$$

where

$$e_{22} = \frac{\sqrt{\omega_p} - \sqrt{\omega_a}}{\sqrt{\omega_p} + \sqrt{\omega_a}}. \quad (3)$$

We used the orbital frequency of the $\ell = 2$, $m = 2$ multipole moments of the gravitational-wave signal.

In order to characterize the eccentricity as a function of time, we associate this eccentricity with a frequency that is an average of the pericenter and apocenter frequencies. This method of computing eccentricity using the waveform itself is advantageous because (i) it enables us to compute the evolution of eccentricity as a function of time (and frequency); (ii) it is gauge independent; and (iii) this definition can be uniformly applied to all waveform models and can be computed during post-processing. We quote eccentricity values at 15 Hz gravitational-wave emission frequency unless specified otherwise. We choose this specific value as this is approximately the low-frequency limit of LIGO–Virgo network’s sensitivity, and is therefore of the order of the initial frequency of detected gravitational-wave signals. This also compares well to the frequency at which eccentricity is typically quoted by different astrophysical models (usually defined at a gravitational-wave emission frequency of $\sim 10 - 15$ Hz ; e.g., Fragione & Bromberg 2019; Zevin et al. 2021).

2.2. Eccentric waveforms

There are multiple ongoing efforts to develop a comprehensive set of eccentric binary coalescence waveforms. Multiple waveform families have been generated using the semi-analytical effective-one-body formalism, which are currently restricted to non-precessing spins (Nagar et al. 2021; Ramos-Buades et al. 2022). A suite of numerical relativity simulations have also been carried out that cover virtually the full eccentric and spin parameter space (Gayathri et al. 2022; Healy & Lousto 2022).

For our analysis, we adopted 12 state-of-the-art numerical relativity waveforms from the Simulating eXtreme Spacetimes (SXS) Collaboration (Hinder et al. 2018; Boyle et al. 2019), which were the only high-fidelity waveforms available to us at the time of this study. These waveforms cover the eccentricity space up to 0.3 defined at 15 Hz gravitational-wave frequency, and include a range of mass ratios: $q \equiv m_2/m_1 = \{1, 0.5, 0.33\}$, where m_2 and m_1 are the lighter and heavier masses, respectively.

As the numerical relativity simulations were carried out for the late stage of the binary coalescence, they cover the gravitational waveform for the full frequency band of the ground-based detectors only for total binary source masses $\gtrsim 70 M_\odot$. Above this mass limit any binary mass can be obtained by a simple scaling of the simulated waveforms due to the scale invariance of general relativity (Tiglio & Villanueva 2021). The selected waveforms are non-spinning, which has limited effect on the sensitivity estimates we compute be-

q	e	Waveform ID
0.33	0.08	SXS:BBH:1371
0.33	0.12	SXS:BBH:1372
0.33	0.27	SXS:BBH:1374
0.5	0.09	SXS:BBH:1365
0.5	0.14	SXS:BBH:1366
0.5	0.29	SXS:BBH:1369
0.5	0.30	SXS:BBH:1370
1.0	0.06	SXS:BBH:1355
1.0	0.14	SXS:BBH:1357
1.0	0.22	SXS:BBH:1361
1.0	0.29	SXS:BBH:1362
1.0	0.30	SXS:BBH:1363

Table 1. Parameters of the 12 numerical relativity simulations adopted from the SXS binary black hole simulations catalog (Boyle et al. 2019). Columns show the binary’s mass ratio q , and eccentricity e at a reference emission frequency of 15 Hz (Section 2.1) for a binary source total mass of $90M_{\odot}$. Spin amplitudes χ_1 and χ_2 are zero for all considered models.

low. When reconstructing the properties of detected gravitational-wave signals, it is important to include spins, as eccentricity and spin precession can mimic each other (Calderón Bustillo et al. 2021; Romero-Shaw et al. 2023). Since we do not use these waveforms to reconstruct properties of signals in this analysis, this problem is not relevant here. We list the properties of the waveforms in Table 1. Figure 1 shows the change in signal morphology as the orbital eccentricity is changed while keeping other source parameters fixed.

We used this set of 12 numerical relativity waveforms to quantify the search sensitivity to high-mass ($\gtrsim 70 M_{\odot}$) eccentric black hole mergers. However, with this limited set of waveforms we could not reconstruct the eccentricity of events.

2.3. Search optimization and sensitivity improvement

Current template-based searches (Cannon et al. 2021; Aubin et al. 2021; Nitz et al. 2017) do not include eccentric gravitational waveforms. As a consequence, their sensitivity is limited for such events, in particular at high eccentricities and low masses (Brown & Zimmerman 2010). Our search was therefore based on the coherent WaveBurst algorithm (cWB; Klimenko et al. 2005; Tiwari et al. 2016; Salemi et al. 2019), which uses minimal assumptions about the signal waveform and hence is expected to be sensitive to eccentric signals.

The cWB algorithm uses the Wilson–Daubechies–Meyer filter to transform time domain detector data to time–frequency representations (Necula et al. 2012).

Excess power regions in the time–frequency representation of strain data that are obtained from the network of detectors are then identified by cWB using clustering algorithms. Selected clusters with excess energy above the expected detector noise are identified as events. The signal waveform, sky coordinates and waveform polarization of the source are then reconstructed for these events using maximum-likelihood analysis (Klimenko et al. 2016).

Once the search pipeline is run, thresholds are placed by cWB on the coherent statistics that it derives for each candidate event. These are used to better differentiate between astrophysical signals and noise artifacts (Gayathri et al. 2019). We will refer to these thresholds on cWB statistics as vetoes. Vetoes define a part of the parameter space over the coherent statistics that should be excluded from the analysis due to the high rate of non-Gaussian noise artifacts there. To maximize the sensitivity of cWB to eccentric binaries, we carried out an optimization of these vetoes applied by cWB to each event. The first two sets of vetoes that are common to the standard cWB pipeline and the eccentric search pipeline are summarized in Appendix A.

Transient non-Gaussian noise artifacts, also known as *glitches*, can limit the detector’s sensitivity to gravitational-wave signals. Targeted vetoes are placed by the standard cWB pipeline to mitigate this problem. These glitch-focused vetoes are derived using cWB summary statistics Q_a and TF . The waveform shape parameter derived by cWB is denoted by Q_a , and is a function of another cWB parameter Q_{veto} ($Q_a = \sqrt{Q_{\text{veto}}}$). This parameter quantifies how well the total energy of the signal is distributed across time (Vedovato 2018; Gayathri et al. 2019; Mishra et al. 2021). The threshold $Q_a > 0.3$ is placed to better distinguish between gravitational waves and a class of low-frequency transient noise artifacts called Blip glitches (Cabero et al. 2019; Davis et al. 2021). Signals due to Blip glitches, which have most of their energy localized to a small time segment have low Q_a values as opposed to signals from binary coalescence, which have higher Q_a values as a consequence of signal energy being distributed over a longer duration. The TF parameter is a function of the signal bandwidth, duration, and power which are additional statistics that cWB estimates for candidate events. A threshold on this parameter is placed to ensure that short-duration glitches that mimic gravitational-wave signals from intermediate mass binary black hole systems are removed.

We injected simulated gravitational-wave signals from equal mass, almost head-on systems (Healy & Lousto 2022) into real detector data to find the set of vetoes that do not remove highly eccentric signals while still reject-

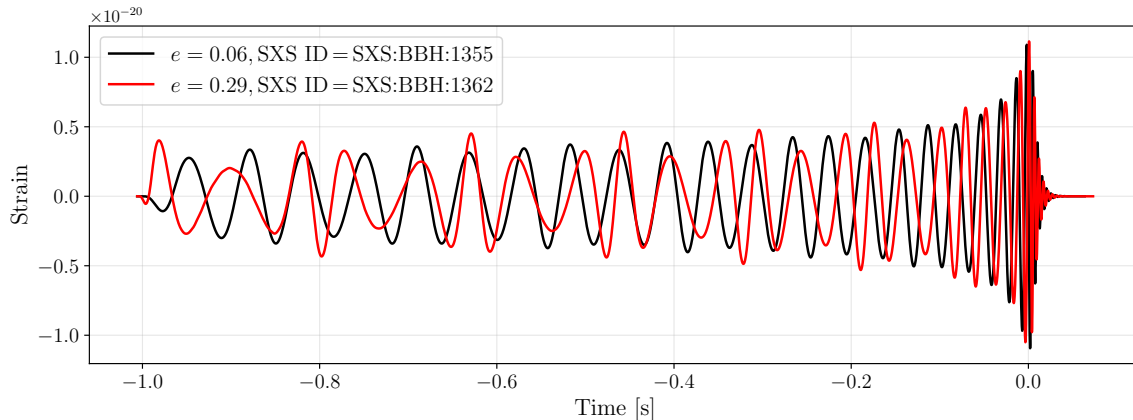


Figure 1. Examples of time-domain waveforms with two different eccentricities (indicated in the legend) for equal mass binary systems with total source mass of $90 M_{\odot}$ at a distance of 100 Mpc. The simulations start at an orbital separation that translates to an orbital frequency $f_{\text{low}} = 15$ Hz. The eccentricity values indicated in the legend are defined at the same f_{low} .

ing most noise artifacts. To perform this optimization, the cWB algorithm was used to detect these injected signals and derive their properties. Vetoes were selected such that they maximized the number of detections at fixed false alarm rates.

We observed that Q_a and TF vetoes were prone to removing a significant fraction of highly eccentric simulated signals. We found that we could mitigate this problem if we removed these two thresholds, and instead introduced a new Q_a-Q_p veto to better distinguish between signals from highly eccentric binaries and short-duration glitches. This veto removes events identified by cWB that do not satisfy the condition $Q_a(Q_p - 0.8) > 0.07$. The summary statistic Q_p quantifies the number of cycles in the reconstructed signal. The Q_a-Q_p veto along with the first two sets of vetoes from the standard search which are summarized in Appendix A were selected as the set of post-production vetoes for the eBBH search. We will refer to this version of cWB that is optimized to eccentric mergers as cWB-eBBH. While the vetoes were optimized using equal-mass waveforms, we confirmed that the optimized search improved eccentric event recovery for unequal mass injections as well.

Figure 2 shows an example of the standard-cWB Q_a veto and the new cWB-eBBH Q_a-Q_p veto for quasi-circular and highly eccentric systems. We also look at this veto’s performance with background events. To generate background events, data from one detector is time-shifted relative to the other detector’s data by an amount greater than the maximum time for a gravitational wave signal to travel between the detectors (Abbott et al. 2016d). The standard veto does well in removing background events and recovering the majority of quasi-circular simulation events. However, the distribution of simulation signals in the Q_a-Q_p space changes

for highly eccentric systems and as a consequence, the standard cWB veto removes a significant fraction of simulation events.

We characterize the sensitivity improvement due to the optimization procedure by computing the number of injected gravitational waves detected by cWB-eBBH but not by standard cWB, divided by the total number of detections by standard cWB. Here we consider a signal detected if it corresponds to an inverse false alarm rate (IFAR) of ≥ 1 yr. This IFAR threshold of ≥ 1 yr was only used to assess the improvement in sensitivity from the introduction of the cWB-eBBH veto, and not as a general detection threshold.

The fraction of events recovered with IFAR ≥ 1 yr by cWB-eBBH that are removed by the standard pipeline with respect to the total number of events recovered by the standard pipeline is $\sim 28\%$ for head-on collision (highly eccentric) equal mass systems with a source total mass of $150 M_{\odot}$. Additionally, we see that this fraction is higher ($\sim 34\%$) for systems with more unequal mass. Therefore, our optimization is the most significant for highly eccentric binaries with unequal masses. The performance of cWB-eBBH for low eccentricity signals remains comparable (within 5%) to the standard pipeline. We conclude that the cWB-eBBH veto does significantly better than the standard veto to improve sensitivity for highly eccentric systems without degrading sensitivity to less eccentric systems.

3. RESULTS

3.1. Search sensitivity

We carried out a search for simulated gravitational-wave signals to quantify the sensitivity of the cWB-eBBH search algorithm. We performed injections in offline (high-latency) re-calibrated O3 strain data with

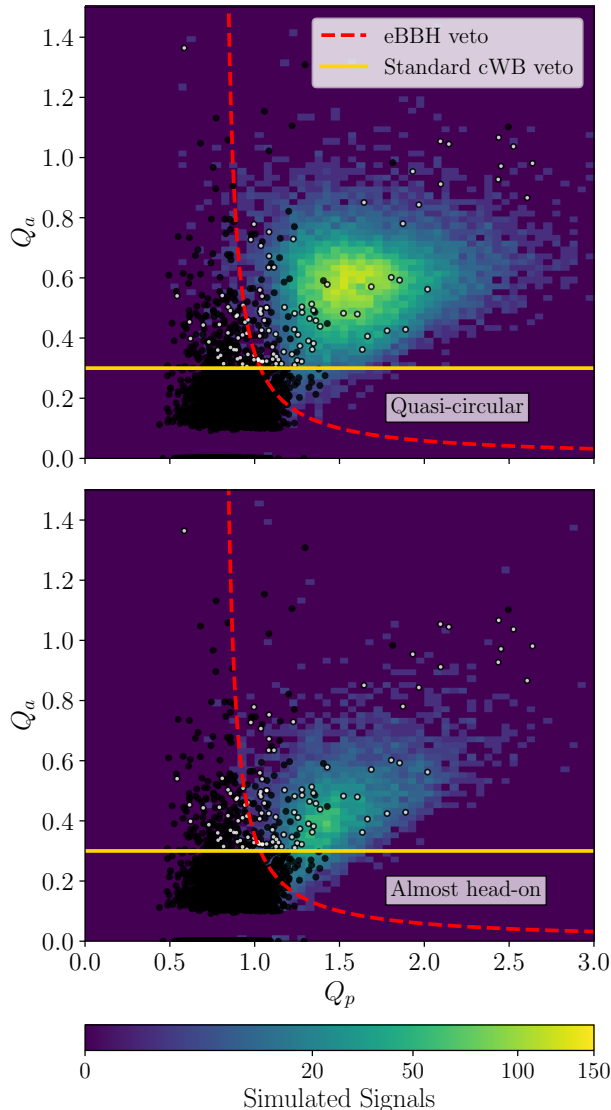


Figure 2. Distribution of Q_a and Q_p for simulated signals (shown as two-dimensional histogram with colorbar denoting number of events in each two-dimensional bin) and loud simulated background events (shown as black dots). The cWB statistics Q_a and Q_p describe the morphology of a signal. The yellow line represents the standard cWB Q_a veto and the red dashed line denotes the eBBH Q_a - Q_p veto. The white dots correspond to loud background events that remain after all standard cWB vetoes (Lopez et al. 2022) are applied. *Top*: Simulated signals correspond to equal mass, source total mass, $M = 150 M_\odot$, quasi-circular orbit systems. *Bottom*: Simulated signals correspond to equal mass, $M = 150 M_\odot$, almost head-on (highly eccentric) systems.

category 0, 1, 2 and 4 data-quality vetoes (Davis et al. 2021; Abbott et al. 2021a). Category 0 vetoes are applied to ensure that the segments of data used in this analysis were collected when the detectors were in observing mode. Category 1 vetoes are used to discard

data from periods in which the detectors were running in an improper configuration, data-dropout or on-site maintenance occurred at either detector, or when there are major problems with the operation of an instrument at the detectors. Category 2 vetoes flag data segments that likely contain non-Gaussian noise artifacts. Category 4 vetoes flag data segments that contain hardware injections. The injected waveforms have source total mass $M \in [70 M_\odot, 200 M_\odot]$. We used the possible 12 configurations of e and q , with 6 choices of source total mass for each of these configurations. Waveforms with different masses were obtained by scaling each of the 12 numerical relativity waveforms listed in Table 1. The simulated signals for each fixed set of source parameters of (M, e, q) were uniformly distributed in sky location (θ, ϕ) and inclination ι . They were also distributed uniformly in co-moving volume up to a maximum redshift z_{\max} . For each waveform, we separately calculated z_{\max} up to which they must be injected so that we do not make unnecessary injections that the search cannot detect. This was calculated with an optimal two-detector-network (Livingston–Hanford) signal-to-noise-ratio threshold of 5.0. Since we observe signals with redshifted mass (Krolak & Schutz 1987), it is in principle possible to inject simulations with total source mass $< 70 M_\odot$ if we populate them at higher redshifts. This was however not performed in the presented analysis. Injections spaced uniformly in time approximately every 100 s in the O3 dataset.

We used the fraction of detected and injected waveforms to compute the sensitive distance of the search for the given waveform. Sensitive distance (Abbott et al. 2019) is defined such that a detector that detects every event within the sensitive distance and no event beyond, it would have the same detection rate as our detector network.

A similar analysis was carried out with data from the first two observing runs of LIGO–Virgo using approximate eccentric waveform models (Abbott et al. 2019). This analysis spanned the binary mass parameter space from $10 M_\odot$ to $100 M_\odot$ while the analysis described in this paper covers binary mass of $70 M_\odot$ to $200 M_\odot$. The sensitivities reported in this paper are higher than that analysis due to increased sensitivity of the detector during the third observing run, and due to the higher masses considered here. There have also been studies to characterize the effect of eccentricity in the sensitivity of long-duration signals with unmodeled search pipelines using hybrid inspiral–merger–ringdown waveform models (Abbott et al. 2021c). However, these studies were targeted towards low mass binary black holes and binary neutron stars as opposed to our search, which is

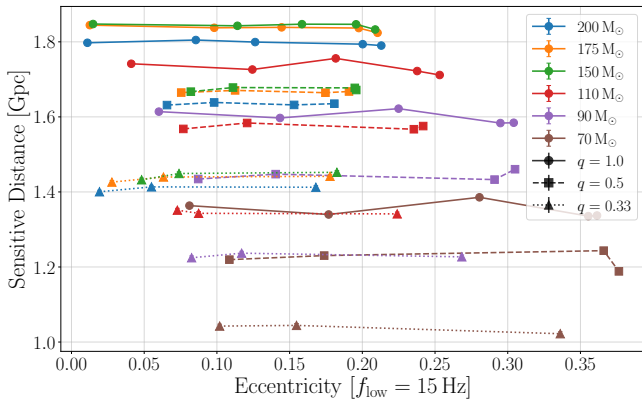


Figure 3. Sensitive distance as a function of orbital eccentricity for different binary total masses and mass ratios. Different marker shapes represent systems with different mass ratios and the different colors represent the various total masses considered here. We used an IFAR threshold of 1.32 yr, which was the loudest new candidate’s IFAR. The horizontal axis denotes the eccentricity of the binary at an orbital separation that corresponds to a frequency of 15 Hz. The statistical error bars on the obtained sensitive distance are smaller than can be presented on this plot.

targeted towards high mass eccentric binaries. Therefore, the search sensitivities reported in Abbott et al. (2021c) are lower than what we obtain in this paper.

The obtained sensitive distance is shown in Figure 3, for different source total masses and mass ratios, as a function of binary eccentricity. The statistical error bars for the obtained sensitive distance range between 0.21 Mpc and 5.63 Mpc. We see that the sensitivity at the considered high masses is mostly independent of the eccentricity up to our highest eccentricity of 0.3. We also see, as expected, that sensitivity is highest for equal mass binaries, and gradually drops as the difference between the two black hole masses increases.

3.2. Search and loudest event

We carried out the cWB-eBBH search over the third observing run of the LIGO and Virgo detectors. For most of the observing run we used data from only the two LIGO detectors, as search sensitivity was not appreciably affected by the addition of Virgo data. For the January 4, 2020 to January 22, 2020 period we also incorporated Virgo in the search to analyze the candidate 200114.020818, which was found by the intermediate mass black hole binary search (Abbott et al. 2022) in the three detector network configuration comprising the LIGO and Virgo detectors. Follow-up studies for this event (Abbott et al. 2022, Appendix B) showed inconsistent results under a quasi-circular binary black hole hypothesis. We investigated if this candidate had higher significance under the eccentric hypothesis. However,

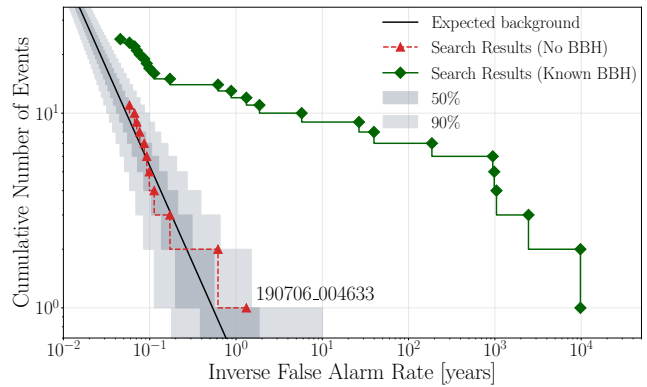


Figure 4. Cumulative number of events as a function of IFAR recovered by the cWB-eBBH search. The solid line represents the expected background for the O3 search, and the gray regions correspond to the 50% and 90% Poisson uncertainty regions. Green squares denote previously reported gravitational-wave candidates (Abbott et al. 2021a; Abbott et al. 2022) recovered by our search, and red triangles show events that were not previously reported by other searches.

this candidate was removed by the cWB-eBBH vetoes. The search and sensitivity results presented below were obtained using data from only the two LIGO detectors.

Our search recovered 28 gravitational-wave candidates with IFAR > 1 yr. By choosing this IFAR threshold, we eliminate low significance candidates that could have been due to noise artifacts in the detector. All but one of these events have been identified previously by other searches as well (Abbott et al. 2021a; Abbott et al. 2022). The results of our search are summarized in Figure 4. The search results excluding previously found candidates is consistent with background noise.

We identified one event candidate with an IFAR > 1 yr that was not previously reported. This most significant new candidate, hereafter referred to as 190706.004633, was observed on July 6, 2019. It was recovered with an IFAR of 1.32 yr. It has an SNR of 12.2 and a central frequency of 74 Hz. Figure 5 shows the time–frequency map of this event candidate.

In order to better understand whether 190706.004633 is of astrophysical origin, we carried out a detailed study of the detector performance and characteristics at the time of the event. This study was aimed to uncover signs of instrumental or environmental artifacts that could have altered the gravitational wave data and hence produced the candidate (Davis et al. 2021, Section 3.2.4). No such artifacts were found. However, the Gravity Spy machine learning classifier (Zevin et al. 2017; Soni et al. 2021) classified the excess power in LIGO Livingston as a Tomte glitch. Tomtes are a common glitch class that are similar in morphology to high-mass binary coalescence signals (Ashton et al. 2022). No glitch or signal

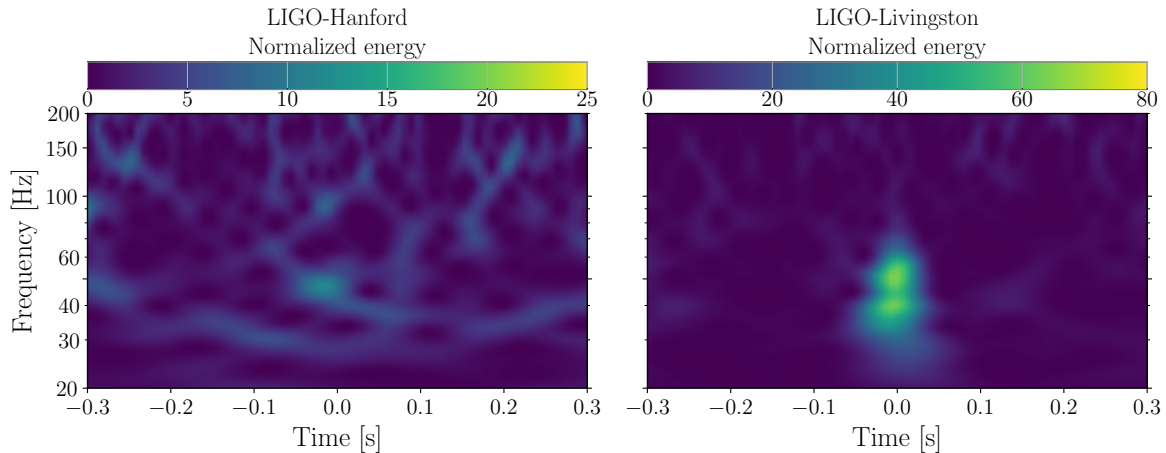


Figure 5. Time-frequency map (spectrogram) of the most significant new candidate identified by the cWB-eBBH search. We show the spectrogram for the LIGO-Hanford (left) and LIGO-Livingston (right) detectors. The individual detector SNRs in the LIGO-Hanford and LIGO-Livingston are 5.6 and 10.9 respectively. Since the energies in the two detectors are very different, we use different scales on the colorbar. The Virgo detector was in observing mode during the time of this event. We used data from all three detectors for follow-up studies and observed that the SNR in the Virgo detector for this event was low (~ 2).

was identified in the LIGO Hanford data by the same classifier. However, as the Gravity Spy machine learning model is not designed to search for astrophysical signals (Glanzer et al. 2023) or to differentiate eccentric binary black hole merger signals from glitches, we cannot rule out an astrophysical origin.

To further investigate this event we carried out a standard parameter estimation analysis of the data using LALInference (Veitch et al. 2015) with nested sampling assuming a quasi-circular waveform. We investigated properties of this event using data from the two LIGO detectors as well as the Virgo detector. For this analysis, in lieu of an eccentric waveform that fully covers the necessary parameter space, we adopted the quasi-circular binary approximant IMRPhenomXPHM (Pratten et al. 2021). This estimation found that the estimated source total mass of 190706.004633 is $M \sim 320 M_{\odot}$, and its estimated redshift is $z \sim 0.3$. Studies have shown that the chirp mass of a binary with low to moderate eccentricity can be reconstructed with a bias of up to 4% using parameter estimation with quasi-circular waveforms (O’Shea & Kumar 2021). However, the reconstructed parameters would be considerably more inaccurate if the signal originated from a highly eccentric binary. Therefore, these results indicate that the signal, if astrophysical, would correspond to a high-mass binary, but should not be used to give precise indications of source properties.

Although astrophysical origin could not be ruled out, we conclude from the large difference measured in the LIGO Hanford and Livingston SNRs that this event is in accordance with an incoherent noise origin rather than

a binary black hole origin. In the following section we therefore compute upper limits to merger rates assuming non-detection of any eccentric event.

4. ECCENTRIC BINARY POPULATION MODELS

In order to understand the astrophysical implications of our results, we computed the expected number of detections for a fiducial source model. For this we adopt the joint total mass and mass ratio probability density $p(M, q)$ which was found to be the best fit for LIGO–Virgo’s observations listed in the GWTC-3 catalog (Abbott et al. 2021a; Abbott et al. 2023) assuming the Power Law + Peak model described in Abbott et al. (2021a). As we have waveforms and simulations that are sparsely sampled in mass and mass ratio, we linearly interpolated the sensitivity of the existing waveforms to points in between the available points in order to obtain a sensitive distance for any source total mass and mass ratio within $70 M_{\odot} \leq M \leq 200 M_{\odot}$ and $0.33 < q < 1.0$. For a more general distribution, we considered a power-law black hole mass distribution of $M^{-2.3}$ (assuming a Salpeter initial mass function; Perna et al. 2019) and a uniform distribution in mass ratio. We further adopted an eccentricity distribution in which the probability density of the binaries’ eccentricity is $p(e) \propto 2(1 - e)$. This distribution is chosen to characterize a population which has a larger fraction of low eccentric binaries.

Having defined the probability density of our fiducial population with respect to the binary parameters, using the sensitive distance obtained over the considered parameter space (see Section 3.1), we computed the total volume–time VT (Abbott et al. 2019, Appendix A) cov-

ered by our search during O3, assuming an IFAR threshold of 1.32 yr, which is the IFAR of our search’s loudest new event. For our fiducial model, we obtained $VT = 6.88 \text{ Gpc}^3 \text{ yr}$ for eccentric binaries with $0 < e < 0.3$. Assuming non-detection of any eccentric event, this would correspond to a constraint of $< 0.33 \text{ Gpc}^{-3} \text{ yr}^{-1}$ on the merger rate density at 90% confidence level in the $70 M_{\odot} \leq M \leq 200 M_{\odot}$ and $0.33 < q < 1.0$ parameter space.

With the small number of available eccentric waveforms for this study, we cannot determine if discovered binaries are eccentric. Therefore, we cannot discount the possibility that previously identified gravitational-wave candidates originate from eccentric binaries. In this case, the number of observed eccentric binaries is greater than zero, and so the merger rate could potentially be higher than our upper limits. Conversely, for some parts of the parameter space, template-based searches have better sensitivities, although we expect them to lose sensitivity at higher eccentricities. Hence, including the VT from these searches (Abbott et al. 2021b; Abbott et al. 2021a) would tighten our upper limits. For simplicity, we limit our results to those from the cWB-eBBH analysis assuming all previously identified candidates are from quasicircular binaries.

Since binary mergers from dynamical formation channels can follow a mass distribution different from the one obtained from GWTC-3, we additionally computed VT assuming other parameter distributions. We summarize our results in Table 2. Our focus on high-mass, eccentric events can be particularly interesting for astrophysical formation channels that favor the production of both high mass and high eccentricity, such as gas-driven capture in AGN disks. For this scenario we adopted the AGN model of Gayathri et al. (2021) as an illustrative example. Our search sensitivity for this model is marginally higher than for the GWTC-3 distribution because this model favors higher masses that are more likely to fall in the mass interval that we are most sensitive to in this analysis. Assuming non-detection of any eccentric event, we place a constraint of $< 0.29 \text{ Gpc}^{-3} \text{ yr}^{-1}$ on the merger rate density at 90% confidence level for AGN-assisted mergers. Taking an estimated $\sim 70\%$ of mergers being eccentric (Samsing et al. 2022) and $\sim 4\%$ of mergers having $M > 70 M_{\odot}$ (Gayathri et al. 2021), we project the corresponding upper limit on the merger rate density to obtain upper limits on the overall AGN-assisted merger rate density as $\sim 0.29 \text{ Gpc}^{-3} \text{ yr}^{-1} / (0.7 \times 0.04) \sim 10.4 \text{ Gpc}^{-3} \text{ yr}^{-1}$. This is consistent with rate estimates in the literature (e.g., Yang et al. 2019; Gayathri et al. 2021).

As a second illustrative model we used the distribution expected in dense star clusters (DSC), adopted from Zevin et al. (2021). For this population, we are able to place a constraint of $< 0.34 \text{ Gpc}^{-3} \text{ yr}^{-1}$ on the merger rate density at 90% confidence level assuming non-detection of any eccentric event. Taking an estimated $\sim 10\%$ being eccentric and $\sim 18\%$ of mergers having $M > 70 M_{\odot}$, we project the corresponding upper limit on the merger rate density to obtain upper limits on the overall DSC-assisted merger rate density as $\sim 0.34 \text{ Gpc}^{-3} \text{ yr}^{-1} / (0.1 \times 0.18) \sim 18.9 \text{ Gpc}^{-3} \text{ yr}^{-1}$. This is consistent with rate estimates in the literature (Kremer et al. 2020; Zevin et al. 2021).

$p(M)$	$p(q)$	$p(e)$	VT [$\text{Gpc}^3 \text{ yr}$]
GWTC-3	GWTC-3	$2(1 - e)$	6.88
GWTC-3	GWTC-3	uniform	6.93
$M^{-2.3}$	uniform	$2(1 - e)$	8.22
$M^{-2.3}$	uniform	uniform	8.27
AGN	AGN	$2(1 - e)$	7.85
AGN	AGN	uniform	7.91
DSC	DSC	DSC	6.69

Table 2. Total volume–time covered by cWB-eBBH search assuming various source total mass, mass ratio, and eccentricity probability density functions for the different illustrative models described in Section 4.

5. CONCLUSION

We carried out a search that does not rely on template banks, and optimized it to be sensitive to high-mass ($M > 70 M_{\odot}$) eccentric binary black hole coalescences. We characterized the sensitivity for this search to understand our findings’ implications for possible eccentric astrophysical populations. Our conclusions are as follows:

1. We did not identify any high significance candidate that was not already detected by other searches. Our loudest and most significant new event has an IFAR of 1.32 yr. We performed detailed follow-up for this event, and concluded that astrophysical origin could not be ruled out. However, our search results are consistent with the expected background for O3.
2. For our fiducial model, we adopted a mass distribution that assumes a Power Law + Peak model and best fits the observations listed in the GWTC-3 catalog. We also chose an eccentricity distribution (defined in Section 4) that favors

quasi-circular binaries. For this assumed population, our search sensitivity is such that assuming non-detection of eccentric events, we can place a constraint of $< 0.33 \text{ Gpc}^{-3} \text{ yr}^{-1}$ on the merger rate density at 90% confidence level. This obtained overall sensitivity is similar to that of other searches for circular black hole mergers in a similar mass range (cf. inferred rate of $0.08^{+0.19}_{-0.07} \text{ Gpc}^{-3} \text{ yr}^{-1}$ of mergers similar to GW190521; Abbott et al. 2022).

3. As an illustrative example, we found that non-detection of any eccentric event corresponds a constraint of $< 10.4 \text{ Gpc}^{-3} \text{ yr}^{-1}$ on the AGN-assisted merger rate density, consistent with rate estimates in the literature (e.g., Yang et al. 2019; Gayathri et al. 2021).
4. As a second illustrative model, we computed our search sensitivity to mergers in dense star clusters, considering the model of Zevin et al. (2021). The results are similar to the AGN channel and our expected sensitivity for a generic eccentric model. For this model, we found that non-detection of eccentric events corresponds to a constraint of $< 18.9 \text{ Gpc}^{-3} \text{ yr}^{-1}$ on the merger rate density, consistent with rate estimates in literature (Kremer et al. 2020; Zevin et al. 2021).

The constraints we place on the rate of eccentric binary coalescences in this work are significantly improved over those computed with data obtained from the first and second observing runs (Abbott et al. 2019). This improvement can be attributed to increased sensitivity of the detectors, progress in the development of highly accurate eccentric waveforms in the high mass domain, and an optimized eccentric search. In view of the expected sensitivity of the fourth observing run by LIGO–Virgo–KAGRA (Abbott et al. 2018), we anticipate to see a significant rise in the number of binary black hole detections. This increases our prospects of detecting gravitational-wave signals from eccentric binary coalescences. Regardless, a non-detection would enable us to further constrain the binary black hole merger rates in astrophysical models favouring eccentric orbits.

Future works will need to expand the study to eccentricities greater than 0.3, and to include masses below $70 M_{\odot}$ as well as black hole spins.

Data-quality products and event-validation results were computed using the DQR Collaboration & Collaboration (2018), DMT John Zweizig (2006), gwdetector Urban et al. (2021), hveto Smith et al. (2011) and iDQ Essick et al. (2020) software packages and contributing

software tools. Analyses in this paper relied upon the LALSuite software library LIGO Scientific Collaboration (2018). The detection of the signals and subsequent significance evaluations in this paper were performed with the coherent WaveBurst (cWB) Klimentko et al. (2005, 2016) package. Estimates of the noise spectra and glitch models were obtained using BayesWave Cornish & Littenberg (2015); Littenberg et al. (2016); Cornish et al. (2021). Source-parameter estimation was performed with the LALInference Veitch et al. (2015) library. PESummary was used to post-process and collate parameter-estimation results Hoy & Raymond (2021). Plots were prepared with Matplotlib Hunter (2007) and GWpy Macleod et al. (2021). NumPy Harris et al. (2020) and SciPy Virtanen et al. (2020) were used in the preparation of the manuscript.

This material is based upon work supported by NSF’s LIGO Laboratory which is a major facility fully funded by the National Science Foundation. The authors also gratefully acknowledge the support of the Science and Technology Facilities Council (STFC) of the United Kingdom, the Max-Planck-Society (MPS), and the State of Niedersachsen/Germany for support of the construction of Advanced LIGO and construction and operation of the GEO 600 detector. Additional support for Advanced LIGO was provided by the Australian Research Council. The authors gratefully acknowledge the Italian Istituto Nazionale di Fisica Nucleare (INFN), the French Centre National de la Recherche Scientifique (CNRS) and the Netherlands Organization for Scientific Research (NWO), for the construction and operation of the Virgo detector and the creation and support of the EGO consortium. The authors also gratefully acknowledge research support from these agencies as well as by the Council of Scientific and Industrial Research of India, the Department of Science and Technology, India, the Science & Engineering Research Board (SERB), India, the Ministry of Human Resource Development, India, the Spanish Agencia Estatal de Investigación (AEI), the Spanish Ministerio de Ciencia e Innovación and Ministerio de Universidades, the Conselleria de Fons Europeus, Universitat i Cultura and the Direcció General de Política Universitaria i Recerca del Govern de les Illes Balears, the Conselleria d’Innovació, Universitats, Ciència i Societat Digital de la Generalitat Valenciana and the CERCA Programme Generalitat de Catalunya, Spain, the National Science Centre of Poland and the European Union – European Regional Development Fund; Foundation for Polish Science (FNP), the Swiss National Science Foundation (SNSF), the Russian Foundation for Basic Research, the Russian Science Foundation, the European Commission,

the European Social Funds (ESF), the European Regional Development Funds (ERDF), the Royal Society, the Scottish Funding Council, the Scottish Universities Physics Alliance, the Hungarian Scientific Research Fund (OTKA), the French Lyon Institute of Origins (LIO), the Belgian Fonds de la Recherche Scientifique (FRS-FNRS), Actions de Recherche Concertées (ARC) and Fonds Wetenschappelijk Onderzoek – Vlaanderen (FWO), Belgium, the Paris Île-de-France Region, the National Research, Development and Innovation Office Hungary (NKFIH), the National Research Foundation of Korea, the Natural Science and Engineering Research Council Canada, Canadian Foundation for Innovation (CFI), the Brazilian Ministry of Science, Technology, and Innovations, the International Center for Theoretical Physics South American Institute for Fundamental Research (ICTP-SAIFR), the Research Grants Council of Hong Kong, the National Natural Science Foundation of China (NSFC), the Leverhulme Trust, the Research Corporation, the National Science and Technology Council (NSTC), Taiwan, the United States Department of Energy, and the Kavli Foundation. The authors gratefully acknowledge the support of the NSF, STFC, INFN and CNRS for provision of computational resources.

This work was supported by MEXT, JSPS Leading-edge Research Infrastructure Program, JSPS Grant-in-Aid for Specially Promoted Research 26000005, JSPS Grant-inAid for Scientific Research on Innovative Areas 2905: JP17H06358, JP17H06361 and JP17H06364, JSPS Core-to-Core Program A. Advanced Research Networks, JSPS Grant-in-Aid for Scientific Research (S) 17H06133 and 20H05639, JSPS Grant-in-Aid for Transformative Research Areas (A) 20A203: JP20H05854, the joint research program of the Institute for Cosmic Ray Research, University of Tokyo, National Research Foundation (NRF), Computing Infrastructure Project of Global Science experimental Data hub Center (GSDC) at KISTI, Korea Astronomy and Space Science Institute (KASI), and Ministry of Science and ICT (MSIT) in Korea, Academia Sinica (AS), AS Grid Center (ASGC) and the National Science and Technology Council (NSTC) in Taiwan under grants including the Rising Star Program and Science Vanguard Research Program, Advanced Technology Center (ATC) of NAOJ, and Mechanical Engineering Center of KEK.

We would like to thank all of the essential workers who put their health at risk during the COVID-19 pandemic, without whom we would not have been able to complete this work.

APPENDIX

A. POST-PRODUCTION VETOES

In this appendix, we will describe in detail the post-production vetoes that are applied by the standard cWB pipeline (Gayathri et al. 2019; Lopez et al. 2022) to distinguish between true gravitational-wave signals and non-Gaussian noise artifacts that can mimic gravitational-wave signals.

The first set of vetoes are based on the morphology of the reconstructed signals. These vetoes are applied to the following cWB summary statistics: the energy-weighted central frequency of the signal f_0 ; \mathcal{M}^* which is the reconstructed chirp mass parameter is obtained by fitting the signal with the characteristic time–frequency evolution for a quasi-circular binary ($f \propto (t - t_c)^{-3/8}$), and Q_a , the waveform shape parameter introduced in Section 2.3. Q_a is a function of the cWB parameter Q_{veto} (Vedovato 2018; Gayathri et al. 2019; Mishra et al. 2021), which quantifies how well the total energy of the signal is distributed across time. The first set of vetoes removes events that do not satisfy $24 \text{ Hz} < f_0 < 100 \text{ Hz}$, $|\mathcal{M}^*/M_\odot| > 10$, $|(\mathcal{M}^*/M_\odot)/Q_a^2| > 15$, $\mathcal{M}^*/M_\odot > -100$.

The next set of vetoes are based on cWB reconstruction, and the correlation of the event across the network of detectors. The cWB summary statistics involved in this set are: norm, defined as the ratio between the total energy over all wavelet resolution levels used for the analysis and the reconstructed energy of the event; χ^2 , a parameter that quantifies the quality of signal reconstruction by computing the residual noise energy that remains once the reconstructed signal is subtracted from data (Gayathri et al. 2019), and finally the $c_c[0]$ and $c_c[2]$ parameters that describe the correlation of the signal across the network of detectors in time domain and frequency domain, respectively (Tiwari et al. 2015). The second set of vetoes remove candidate events that do not satisfy $\text{norm} > 4$, $\log_{10}(\chi^2) < 0.4$, $c_c[0] > 0.8$, $c_c[2] > 0.7$.

The two sets of vetoes described above were optimized with gravitational waveforms for quasi-circular binary black hole coalescences for the standard cWB pipeline. We found that they performed optimally in recovering eBBH signals as well. Therefore, these vetoes along with the new eBBH veto introduced in Section 2.3 were chosen as the final set of vetoes for the cWB-eBBH search pipeline.

REFERENCES

- Aasi, J., Abbott, B. P., Abbott, R., et al. 2015, *Classical and Quantum Gravity*, 32, 074001
- Abbott, B. P., Abbott, R., Abbott, T. D., et al. 2016a, *PhRvL*, 116, 061102
- Abbott, B. P., et al. 2016b, *PhRvL*, 116, 241102
- . 2016c, *PhRvL*, 116, 221101, [Erratum: *PhRvL*. 121, 129902 (2018)]
- . 2016d, *Class. Quant. Grav.*, 33, 134001
- Abbott, B. P., Abbott, R., Abbott, T. D., et al. 2017, *ApJL*, 848, L12
- Abbott, B. P., et al. 2017a, *Astrophys. J. Lett.*, 848, L13
- . 2017b, *Nature*, 551, 85
- . 2017c, *PhRvL*, 118, 221101, [Erratum: *PhRvL*. 121, 129901 (2018)]
- . 2018, *Living Rev. Rel.*, 21, 3
- Abbott, B. P., Abbott, R., Abbott, T. D., et al. 2019, *ApJ*, 883, 149
- Abbott, B. P., Abbott, R., Abbott, T. D., et al. 2019, *PhRvD*, 100, 064064
- Abbott, R., Abbott, T. D., Abraham, S., et al. 2021a, *ApJL*, 913, L7
- . 2020, *ApJL*, 900, L13
- Abbott, R., et al. 2021b, arXiv:2108.01045
- Abbott, R., Abbott, T. D., Acernese, F., et al. 2021a, arXiv e-prints, arXiv:2111.03606
- Abbott, R., Abe, H., Acernese, F., et al. 2021b, arXiv e-prints, arXiv:2111.03604
- . 2021c, arXiv e-prints, arXiv:2112.06861
- Abbott, R., et al. GWTC-3: Compact Binary Coalescences Observed by LIGO and Virgo During the Second Part of the Third Observing Run — Parameter estimation data release. 2021a
- Abbott, R., et al. 2021b, *SoftwareX*, 100658
- . 2021c, *PhRvD*, 104, 102001
- . 2022, *A&A*, 659, A84
- . 2023, *Phys. Rev. X*, 13, 011048
- Acernese, F., Agathos, M., Agatsuma, K., et al. 2015, *CQGra*, 32, 024001
- Albanesi, S., Nagar, A., & Bernuzzi, S. 2021, *PhRvD*, 104, 024067
- Antonini, F., Toonen, S., & Hamers, A. S. 2017, *ApJ*, 841, 77
- Ashton, G., Thiele, S., Lecoche, Y., McIver, J., & Nuttall, L. K. 2022, *CQGra*, 39, 175004
- Askar, A., Szkudlarek, M., Gondek-Rosińska, D., Giersz, M., & Bulik, T. 2017, *MNRAS*, 464, L36
- Aubin, F., et al. 2021, *CQGra*, 38, 095004
- Baibhav, V., Gerosa, D., Berti, E., et al. 2020, *PhRvD*, 102, 043002
- Banerjee, S., Baumgardt, H., & Kroupa, P. 2010, *MNRAS*, 402, 371
- Bartos, I., Kocsis, B., Haiman, Z., & Márka, S. 2017, *ApJ*, 835, 165
- Bartos, I., Rosswog, S., Gayathri, V., et al. 2023, arXiv e-prints, arXiv:2302.10350
- Belczynski, K., Kalogera, V., & Bulik, T. 2002, *ApJ*, 572, 407
- Bethe, H. A., & Brown, G. E. 1998, *ApJ*, 506, 780
- Boyle, M., et al. 2019, *CQGra*, 36, 195006
- Brown, D. A., & Zimmerman, P. J. 2010, *PhRvD*, 81, 024007
- Buonanno, A., Kidder, L. E., Mroué, A. H., Pfeiffer, H. P., & Taracchini, A. 2011, *PhRvD*, 83, 104034
- Cabero, M., Lundgren, A., Nitz, A. H., et al. 2019, *CQGra*, 36, 155010
- Calderón Bustillo, J., Sanchis-Gual, N., Torres-Forné, A., & Font, J. A. 2021, *Phys. Rev. Lett.*, 126, 201101
- Cannon, K., Caudill, S., Chan, C., et al. 2021, *SoftwareX*, 14, 100680
- Cao, Z., & Han, W.-B. 2017, *Phys. Rev. D*, 96, 044028
- Collaboration, L. S., & Collaboration, V. Data quality report user documentation, docs.ligo.org/detchar/data-quality-report/. 2018
- Cornish, N. J., & Littenberg, T. B. 2015, *Class. Quant. Grav.*, 32, 135012
- Cornish, N. J., Littenberg, T. B., Bécsy, B., et al. 2021, *Phys. Rev. D*, 103, 044006
- Cornish, N. J., & Shapiro Key, J. 2010, *PhRvD*, 82, 044028, [Erratum: *PhRvD* 84, 029901 (2011)]
- Davis, D., Areeda, J. S., Berger, B. K., et al. 2021, *CQGra*, 38, 135014
- de Mink, S. E., & Mandel, I. 2016, *MNRAS*, 460, 3545
- Dominik, M., Belczynski, K., Fryer, C., et al. 2013, *ApJ*, 779, 72
- Dominik, M., Berti, E., O’Shaughnessy, R., et al. 2015, *ApJ*, 806, 263
- Essick, R., Godwin, P., Hanna, C., Blackburn, L., & Katsavounidis, E. 2020, *Mach. Learn.: Sci. Technol.*, 2, 015004
- Fishbach, M., Holz, D. E., & Farr, B. 2017, *ApJL*, 840, L24
- Fragione, G., & Bromberg, O. 2019, *MNRAS*, 488, 4370
- Fragione, G., Grishin, E., Leigh, N. W. C., Perets, H. B., & Perna, R. 2019, *MNRAS*, 488, 47
- Gallegos-Garcia, M., Berry, C. P. L., Marchant, P., & Kalogera, V. 2021, *ApJ*, 922, 110
- Gamba, R., Breschi, M., Carullo, G., et al. 2023, *NatAs.*, 7, 11

- Gayathri, V., Bacon, P., Pai, A., et al. 2019, *PhRvD*, 100, 124022
- Gayathri, V., Yang, Y., Tagawa, H., Haiman, Z., & Bartos, I. 2021, *ApJL*, 920, L42
- Gayathri, V., Healy, J., Lange, J., et al. 2022, *NatAs*, doi:10.1038/s41550-021-01568-w
- Gerosa, D., Berti, E., O’Shaughnessy, R., et al. 2018, *PhRvD*, 98, 084036
- Glanzer, J., et al. 2023, *Class. Quant. Grav.*, 40, 065004
- Harris, C. R., et al. 2020, *Nature*, 585, 357
- Healy, J., & Lousto, C. O. 2022, arXiv e-prints, arXiv:2202.00018
- Healy, J., Lange, J., O’Shaughnessy, R., et al. 2018, *PhRvD*, 97, 064027
- Hinder, I., Kidder, L. E., & Pfeiffer, H. P. 2018, *PhRvD*, 98, 044015
- Hinderer, T., & Babak, S. 2017, *PhRvD*, 96, 104048
- Hoy, C., & Raymond, V. 2021, *SoftwareX*, 15, 100765
- Huerta, E. A., Kumar, P., McWilliams, S. T., O’Shaughnessy, R., & Yunes, N. 2014, *PhRvD*, 90, 084016
- Hunter, J. D. 2007, *Comput. Sci. Eng.*, 9, 90
- Inayoshi, K., Hirai, R., Kinugawa, T., & Hotokezaka, K. 2017, *MNRAS*, 468, 5020
- Islam, T., Varma, V., Lodman, J., et al. 2021, *PhRvD*, 103, 064022
- John Zweizig. The Data Monitor Tool Project, labcit.ligo.caltech.edu/~jzweizig/DMT-Project.html. 2006
- Junker, W., & Schaefer, G. 1992, *MNRAS*, 254, 146
- Khalil, M., Buonanno, A., Steinhoff, J., & Vines, J. 2021, *PhRvD*, 104, 024046
- Klimenko, S., Mohanty, S., Rakhmanov, M., & Mitselmakher, G. 2005, *PhRvD*, 72, 122002
- Klimenko, S., Vedovato, G., Drago, M., et al. 2016, *PhRvD*, 93, 042004
- Kozai, Y. 1962, *AJ*, 67, 591
- Kremer, K., Ye, C. S., Rui, N. Z., et al. 2020, *Astrophys. J. Suppl.*, 247, 48
- Krolak, A., & Schutz, B. F. 1987, *General Relativity and Gravitation*, 19, 1163
- Lenon, A. K., Brown, D. A., & Nitz, A. H. 2021, *PhRvD*, 104, 063011
- Lewis, A. G. M., Zimmerman, A., & Pfeiffer, H. P. 2017, *CQGra*, 34, 124001
- Lidov, M. L. 1962, *Planet. Space Sci.*, 9, 719
- LIGO Scientific Collaboration. LIGO Algorithm Library, doi.org/10.7935/GT1W-FZ16. 2018
- LIGO Scientific Collaboration, Virgo Collaboration and KAGRA Collaboration. GWTC-3 Data Release, www.gw-openscience.org/GWTC-3/. 2021
- Littenberg, T. B., Kanner, J. B., Cornish, N. J., & Millhouse, M. 2016, *Phys. Rev. D*, 94, 044050
- Liu, X., Cao, Z., & Zhu, Z.-H. 2022, *Class. Quant. Grav.*, 39, 035009
- Lopez, D., Gayathri, V., Pai, A., et al. 2022, *PhRvD*, 105, 063024
- Loutrel, N., Liebersbach, S., Yunes, N., & Cornish, N. 2018, *CQGra*, 36, 025004
- Macleod, D., et al. [gwpv/gwpv, doi.org/10.5281/zenodo.597016](https://doi.org/10.5281/zenodo.597016). 2021
- Mapelli, M. 2016, *MNRAS*, 459, 3432
- Marchant, P., Langer, N., Podsiadlowski, P., Tauris, T. M., & Moriya, T. J. 2016, *A&A*, 588, A50
- Margutti, R., & Chornock, R. 2021, *Ann. Rev. Astron. Astrophys.*, 59, 155
- Martinez, M. A. S., Fragione, G., Kremer, K., et al. 2020, *ApJ*, 903, 67
- McKernan, B., Ford, K. E. S., Lyra, W., & Perets, H. B. 2012, *MNRAS*, 425, 460
- Mishra, T., O’Brien, B., Gayathri, V., et al. 2021, *PhRvD*, 104, 023014
- Mora, T., & Will, C. M. 2004, *PhRvD*, 69, 104021
- Morscher, M., Pattabiraman, B., Rodriguez, C., Rasio, F. A., & Umbreit, S. 2015, *ApJ*, 800, 9
- Nagar, A., Bonino, A., & Rettegno, P. 2021, *PhRvD*, 103, 104021
- Naoz, S. 2016, *ARA&A*, 54, 441
- Necula, V., Klimentko, S., & Mitselmakher, G. 2012, *J. Phys. Conf. Ser.*, 363, 012032
- Nitz, A. H., Dent, T., Dal Canton, T., Fairhurst, S., & Brown, D. A. 2017, *ApJ*, 849, 118
- O’Shea, E., & Kumar, P. 2021, arXiv:2107.07981
- Perna, R., Wang, Y.-H., Farr, W. M., Leigh, N., & Cantiello, M. 2019, *Astrophys. J. Lett.*, 878, L1
- Peters, P. C. 1964, *PhRv*, 136, B1224
- Peters, P. C., & Mathews, J. 1963, *PhRv*, 131, 435
- Portegies Zwart, S. F., & McMillan, S. L. W. 2000, *ApJL*, 528, L17
- Pratten, G., et al. 2021, *PhRvD*, 103, 104056
- Ramos-Buades, A., Buonanno, A., Khalil, M., & Ossokine, S. 2022, *PhRvD*, 105, 044035
- Ramos-Buades, A., Husa, S., Pratten, G., et al. 2020, *PhRvD*, 101, 083015
- Ramos-Buades, A., van de Meent, M., Pfeiffer, H. P., et al. 2022, *PhRvD*, 106, 124040
- Randall, L., & Xianyu, Z.-Z. 2018, *ApJ*, 853, 93
- Rodriguez, C. L., Chatterjee, S., & Rasio, F. A. 2016a, *PhRvD*, 93, 084029
- Rodriguez, C. L., Zevin, M., Pankow, C., Kalogera, V., & Rasio, F. A. 2016b, *ApJL*, 832, L2

- Romero-Shaw, I., Lasky, P. D., & Thrane, E. 2021, *ApJL*, 921, L31
- Romero-Shaw, I., Lasky, P. D., Thrane, E., & Calderón Bustillo, J. 2020, *ApJL*, 903, L5
- Romero-Shaw, I. M., Gerosa, D., & Loutrel, N. 2023, *MNRAS*, 519, 5352
- Salemi, F., et al. 2019, *PhRvD*, 100, 042003
- Samsing, J., Bartos, I., D’Orazio, D. J., et al. 2022, *Nature*, 603, 237
- Setyawati, Y., & Ohme, F. 2021, *PhRvD*, 103, 124011
- Shaikh, M. A., Varma, V., Pfeiffer, H. P., Ramos-Buades, A., & van de Meent, M. 2023, *arXiv:2302.11257*
- Smith, J. R., Abbott, T., Hirose, E., et al. 2011, *Class. Quant. Grav.*, 28, 235005
- Soni, S., et al. 2021, *Class. Quant. Grav.*, 38, 195016
- Tagawa, H., Haiman, Z., Bartos, I., & Kocsis, B. 2020, *ApJ*, 899, 26
- Tagawa, H., Kocsis, B., Haiman, Z., et al. 2021, *ApJL*, 907, L20
- Tanay, S., Haney, M., & Gopakumar, A. 2016, *PhRvD*, 93, 064031
- Tiglio, M., & Villanueva, A. 2021, *Sci. Rep.*, 11, 5832
- Tiwari, V., Klimenko, S., Necula, V., & Mitselmakher, G. 2015, *CQGra*, 33, 01LT01
- Tiwari, V., Klimenko, S., Christensen, N., et al. 2016, *PhRvD*, 93, 043007
- Urban, A. L., et al. *gwdetchar/gwdetchar*, doi.org/10.5281/zenodo.2575786. 2021
- Vedovato, G. The Qveto algorithm. 2018. <https://gwburst.gitlab.io/documentation/latest/html/faq.html?highlight=qveto#the-qveto>
- Veitch, J., Raymond, V., Farr, B., et al. 2015, *PhRvD*, 91, 042003
- Vigna-Gómez, A., Toonen, S., Ramirez-Ruiz, E., et al. 2021, *ApJL*, 907, L19
- Virtanen, P., et al. 2020, *Nature Meth.*, 17, 261
- Vitale, S., Lynch, R., Sturani, R., & Graff, P. 2017, *Class. Quant. Grav.*, 34, 03LT01
- Wang, H., Zou, Y.-C., & Liu, Y. 2023, *arXiv:2302.11227*
- Wysocki, D., Lange, J., & O’Shaughnessy, R. 2019, *PhRvD*, 100, 043012
- Yang, Y., Bartos, I., Haiman, Z., et al. 2019, *ApJ*, 876, 122
- Zevin, M., Romero-Shaw, I. M., Kremer, K., Thrane, E., & Lasky, P. D. 2021, *ApJL*, 921, L43
- Zevin, M., et al. 2017, *CQGra*, 34, 064003
- Zevin, M., Bavera, S. S., Berry, C. P. L., et al. 2021, *ApJ*, 910, 152
- Ziosi, B. M., Mapelli, M., Branchesi, M., & Tormen, G. 2014, *MNRAS*, 441, 3703